Neurochemistry International 131 (2019) 104581

Contents lists available at ScienceDirect

Neurochemistry International

journal homepage: www.elsevier.com/locate/neuint

Salubrinal attenuates nitric oxide mediated PERK:IRE1α: ATF-6 signaling and DNA damage in neuronal cells

Sonam Gupta[a,b], Joyshree Biswas[a], Parul Gupta[a,b], Abhishek Singh[a], Shubhangini Tiwari[a], Amit Mishra[c], Sarika Singh[a,b,*]

[a] Toxicology and Experimental Medicine Division, CSIR-Central Drug Research Institute, Lucknow, 226031, Uttar Pradesh, India
[b] Academy of Scientific & Innovative Research (AcSIR), Lucknow, 226031, Uttar Pradesh, India
[c] Cellular and Molecular Neurobiology Unit, Indian Institute of Technology Jodhpur, Rajasthan, 342011, India

ARTICLE INFO

Keywords:
Endoplasmic reticulum stress
Nitric oxide
Salubrinal
DNA damage

ABSTRACT

The present study was conducted to investigate the effect of salubrinal on nitric oxide mediated endoplasmic reticulum stress signaling and neuronal apoptosis. Rotenone treatment to neuro2a cells caused significantly decreased cell viability, increased cytotoxicity, augmented nitrite levels, increased nitrotyrosine level and augmented level of key ER stress markers (GRP-78, GADD153 and caspase-12). These augmented levels of ER stress markers could be attenuated with pretreatment of nitric oxide synthase inhibitor-aminoguanidine as well as with salubrinal. The rotenone treatment to neuro2a cells also triggered the ER stress induced up regulation of various signaling factors of unfolded protein response involving pPERK, ATF4, p-IRE1α, XBP-1 and ATF-6. Pretreatment of salubrinal significantly attenuated the activation of transmembrane kinases (PERK and IRE1) and ATF6 and restored the rotenone induced altered level of other UPR related signaling factors. Rotenone induced dephosphorylation of eIF2α was also inhibited with salubrinal treatment. Biochemically rotenone treatment to neuro2a cells caused the reactive oxygen species generation, depleted mitochondrial membrane potential and increased intra cellular calcium level which was attenuated with salubrinal treatment. Rotenone treatment to neuro2a cells also caused neuronal apoptosis, DNA fragmentation and chromatin condensation which were attenuated with salubrinal treatment. In conclusion, the findings suggested that rotenone causes the augmented level of nitric oxide which contributes in ER stress and could be inhibited by both aminoguanidine and/or salubrinal treatment. Further, salubrinal treatment attenuates the nitric oxide induced ER stress axis PERK:IRE1α:ATF-6 and inhibits the DNA damage and neuronal apoptosis.

1. Introduction

Endoplasmic reticulum (ER) stress is the consequence of the perturbation of ER homeostasis which determines the activation of exquisitely regulated event termed as unfolded protein response (UPR) (Yu-Mi Jeon et al., 2017; Chung et al., 2015; Xu et al., 2005). The primary function of UPR is to restore the ER or cellular homeostasis. It could be activated through various physiological as well as pathological responses like hypoxia, glucose deprivation, genome instability and exposure to cytotoxic compounds. UPR activation caused the dissociation of chaperon glucose regulated protein (GRP78) offering the activation of transmembrane kinases and activating transcription factors (Wang et al., 2009). Specifically, these kinases are protein kinase RNA-like ER kinase (PERK), inositolrequiring enzyme 1 (IRE1) and activating transcription factor 6 (ATF6) located on ER membrane. GRP78 dissociation mediated dimerization and activation of PERK causes the phosphorylation of eIF2α to arrest the translation and prevent the cell from apoptosis. However, reports have shown that sustained phosphorylation of eIF2α and translational repression of global protein synthesis takes place during severe or prolonged stressed conditions may lead to synaptic failures in neurodegenerative disease pathology (Ohno, 2014). In response to cellular stressed condition the phosphorylated eIF2α induced translation attenuation takes place but that is coincide with the preferential translation of ATF4 which is a key regulator for the transcription of adaptive genes and may initiate autophagy (B'chir et al., 2013). It has also been reported that ATF4 is a redox regulated prodeath transcriptional activator in response to oxidative stress (Lange et al., 2008). GRP78 dissociation from the IRE1 activates it through its phosphorylation and offers the splicing of X-box-binding protein (XBP1) mRNA to form a transcriptionally active mRNA, named

* Corresponding author. Toxicology and Experimental Medicine Division, CSIR-Central Drug Research Institute, Lucknow, 226031, Uttar Pradesh, India.
E-mail address: sarika_singh@cdri.res.in (S. Singh).

https://doi.org/10.1016/j.neuint.2019.104581
Received 22 May 2019; Received in revised form 9 October 2019; Accepted 15 October 2019
Available online 19 October 2019
0197-0186/

XBP1s (spliced). Spliced XBP1 functions as a transcription factor during endoplasmic reticulum (ER) stress by regulating the unfolded protein response. XBP1s could also promote the cell survival by offering the inhibition of C/EBP homologous protein (CHOP)/growth arrest- and DNA damage-inducible gene 153 (GADD153) expression and regulates the expression of genes involved in secretory pathways and in the expansion of ER compartment (Ron and Hubbard., 2008). The activated PERK pathway alleviates both the synthesis of ATF6 and its trafficking from the ER to the golgi for intramembrane proteolysis and activation of ATF6 (Corazzari et al., 2017). In addition ATF6 could also augment the chaperon expression including GRP78, GRP94, isomerases and SERCA2 to increase the protein folding capacity of ER (Haze et al., 1999; Huang et al., 2006). ER stress also leads to activation of GADD153 which could undergo phosphorylation at Ser78 and Ser81 and evokes maximal apoptotic effect in cell (Oyadomari and Mori., 2004; Nishitoh, 2012). Increased level of GADD153 causes depleted level of antiapoptotic factor Bcl-2 thus further contributes in cellular death (Li et al., 2014). Previously we have reported that rotenone exposure to neuro2a cells caused the altered level of key ER stress markers (Goswami et al., 2014) therefore used in present study.

Rotenone is an environmental toxin, causes neurotoxicity through mitochondrial complex I inhibition and has been used to induce experimental parkinsonism in animals and cell cultures. It causes apoptosis by enhancing the generation of mitochondrial reactive oxygen species (ROS) in cultured cells (Li et al., 2003). Previous studies from our laboratory have reported the rotenone induced oxidative and nitrosative stress-mediated neuronal death (Goswami et al., 2014; Swarnkar et al., 2012). Nitric oxide is a diffusible free radical and inhibits the mitochondrial electron transport chain (ETC) which causes depleted ATP level (Brorson and Zhang, 1997) along with disrupted mitochondrial membrane potential (Brown et al., 2001). Such impaired ETC and depleted ATP level may also contribute to formation of mitochondrial permeability transition pore which further facilitate the release of proapoptotic factors from the mitochondria (Liu et al., 1996; Susin et al., 1999) which is directly related to cellular apoptosis (). Previously also we have shown the role of NO in the impairment of mitochondrial complex-I activity, cytochrome-c efflux and caspase-3 activation in rat brain (Singh et al., 2010). Though salubrinal is selective Inhibitor of eIF2α dephosphorylation thus restore the translation arrest to protect the cell but its antiapoptotic effects are also reported in various test systems (Paschen, 2003; Li et al., 2014; Matsuoka and Komoike, 2015; Boyce et al., 2005; Methippara et al., 2012; Wu et al., 2011; Xiuna Jing et al., 2014; Huang et al., 2012). It also reduces the load of ER located mutant or mislocated proteins of neurons during neuropathological conditions (Liu et al., 2012). The present study was conducted with two main objective – one was to decipher whether the rotenone induced augmented nitrite level could cause the ER stress and second was what are the effect of salubrinal on various signaling factors of UPR. To attain this we have employed the neuro2a cells to rotenone exposure and assessed the various parameters like cell viability, cytotoxicity, mRNA level, protein levels of ER stress signaling markers, chromatin condensation, DNA fragmentation, caspase-3 activity and Annexin V staining for neuronal apoptosis with and without salubrinal/aminoguanidine treatment.

2. Materials and methods

2.1. Reagents and antibodies

Agarose, aminoguanidine and bovine serum albumin were obtained from Sigma chemicals (St. Louis, USA). Copper sulphate ($CuSo_4$), calcium chloride ($Cacl_2$) were purchased from company SRL, India. Dichlorofluorescein diacetate (DCF-DA), disodium hydrogen phosphate, dimethyl sulphoxide (DMSO), ethidium bromide, glucose, 4-(2-hydroxyethyl)-1-piperazineethanesulfonic acid (HEPES), 3–4, 5-dimethylthiazol-2-yl −2,5-diphenyl tetrazolium bromide dye (MTT), low melting agarose, magnesium chloride, Nicotinamide adenine dinucleotide (NADH), propidium iodide, NP-40 and tris buffer were procured from company Sigma, USA. Dulbecco's modified Eagle's medium (DMEM), fetal bovine serum, trizol, Ham's F12 media and penicillin-streptomycin were purchased from company Invitrogen, USA. **Folin-Ciocalteu** reagent, potassium chloride, and ethylene diamine tetra acetic acid (EDTA) were procured from company SRL, India. Di potassium hydrogen orthophosphate (K_2HPO_4), dithiothrietol (DTT), disodium hydrogen phosphate (Na_2HPO_4), ethylene glycol tetra acetic acid (EGTA), potassiumdihydrogen phosphate (KH_2PO_4), reduced nicotine amide adenine dinucleotide phosphate (NADPH), sodium bicarbonate, sodium pyruvate, sodium azide (NaN_3), sodium chloride (NaCl), sodium phosphate (NaH_2PO_4) and rotenone were obtained from Sigma Chemicals (St. Louis, USA). Sodium carbonate, sodium chloride, sodium dihydrogen phosphate, sodium hydroxide, sodium potassium tartarate were procured from company SRL, India. Salubrinal was purchased from Tocris, Bristol, UK. Triton-X-100 was obtained from Sisco Research Laboratories Limited, Mumbai, India. Rhodamine 123, pepstatin, PMSF, protease inhibitor cocktail, fluo-3-AM, mouse monoclonal anti β-actin antibody (Ab) (A5316), rabbit polyclonal anti calnexin Ab (C4731), mouse monoclonal anti caspase-12 Ab (catalog no. C7611), goat polyclonal anti IRE1α Ab (SAB2500366), rabbit polyclonal anti pIRE1α Ab (PR53655) and anti rabbit and mouse HRP secondary Ab (A0544, A0168) were purchased from Sigma (St. Louis, USA). Rabbit polyclonal anti GRP-78 Ab (SC-13968), GADD 153 Ab (SC-575), ATF-6 Ab (SC-166659), ATF-4 Ab (SC-200), XBP-1 Ab (SC-7160), PERK Ab (SC-13073), pPERK Ab (SC-32577), eIF2α Ab (SC-11386), p-eIF2α Ab (SC-293100), mouse monoclonal anti 3- nitrotyrosine Ab (SC-32757), rabbit polyclonal anti histone H3 Ab (SC-10809), mouse anti goat HRP secondary Ab (SC2354) and mouse monoclonal anti caspase-3 Ab (SC-56053) were purchased from Santa cruz (Dallas, Texas USA). PCR 2X master mix were procured from Thermo scientific (MA, USA), high Capacity cDNA reverse transcription kit was purchased from applied biosystems, USA. ECL-Plus detection kit was obtained from Pierce Biosciences (USA). Caspase-3 activity assay detection kit was purchased from Sigma (St. Louis, USA). Annexin V-FITC/PI apoptosis detection kit was obtained from Merck (Millipore).

2.2. Cell culture and treatments

Mouse neuronal cell line neuro2a was acquired from the National Center of Cell Sciences, Pune, India, and maintained using DMEM/F12 (1:1) culture medium with 10% FBS at 37 °C and 5% CO_2. Cells were pretreated with salubrinal (5, 10 and 20 μM) for 1 h. Then, the cells were treated with varied concentrations of rotenone (0.1, 0.5, 1 μM) for 24 h. The dose of salubrinal was finalized on the basis of cell viability data. 5 μM dose of salubrinal exhibited the significant attenuation against rotenone induced decreased cell viability in comparison to control cells therefore used for further experiments. Cells were also co-treated with aminoguanidine [100 μM] (Gupta et al., 2015a,b).

2.3. Cell viability assay

Cell viability was estimated by using 3–4,5-dimethylthiazol-2-yl-2,5-diphenyltetrazolium bromide (MTT) dye as reported previously (Biswas et al., 2016). After treatment, the cells were incubated with MTT dye (100μg/ml) in the dark for 2 h at 37 °C, supernatants were carefully aspirated. The colored formazan crystals were dissolved in DMSO and the absorbance was measured at 550 nm by using spectrophotometer (Eon, Biotek, USA).

2.4. LDH release assay

After treatment the culture medium was collected. The protein was estimated by using Lowry's method (Lowry et al., 1951) and LDH estimation was done by the method described by Wroblewski and Laude

Table 1
Primer sequences and specific conditions for reverse transcriptase PCR.

Gene	Primer sequence	Annealing temp (C^0)	Product size
GRP-78	Forward: 5′-GTTCTGCTTGATGTGTGTCC-3′ Reverse: 5′-TTTGGTCATTGGTGATGGTG-3′	53	349
GADD	Forward: 5′-TCAGATGAAATTGGGGGCAC-3′ Reverse: 5′-TTTCCTCGTTGAGCCGCTCG-3′	57	340
Caspase-12	Forward: 5′-GGCCGTCCAGAGCACCAGT-3′ Reverse: 5′-CAGTGGCTATCCCTTTGCTTG-3′	58	253
Caspase-3	Forward: 5′-AGTGACCATGGAGAACAACA-3′ Reverse: 5′-AGCTGCTCCTTTTGCTATGA-3′	54	347
β-actin	Forward: 5′-GTCGTACCACTGGCATTGTG-3′ Reverse: 5′-CTCTCAGCTGTGGTGGTGAA-3′	56	181

(1955). Briefly the reaction mixture was set up accordingly using 0.1 M sodium phosphate buffer (pH 7.2) and the substrate-sodium pyruvate (1.5 mM). This mixture was incubated at 37 °C for 30 min Reaction was initiated with addition of NADH (0.5 mM), and change in absorbance was measured by spectrophotometer (Eon, BioTek, USA) at 340 nm for 2 min at an interval of 15 s. Activity was calculated in terms of substrate utilized per minute/mg of protein.

2.5. mRNA expression by reverse transcriptase PCR

RNA was isolated using Trizol reagent according to manufacturer's protocol. Concentration of RNA was determined by Nanodrop (Quawell UV–Vis spectrophotometer Q5000, USA). Approximately 2 μg of RNA was used to prepare cDNA using high capacity cDNA reverse transcription kit as per the given protocol in 20 μl of reaction volume. The cDNA was further amplified separately with specific primers for β-actin, GRP-78, GADD153, caspase-12 and caspase-3 using PCR Master mix in Veriti thermal cycler (AB Applied Biosystem). Band intensity was quantified by Image J software (Gupta et al., 2014). Primer sequences and the specifications are provided in Table 1.

2.6. Immunoblotting in subcellular fractionation

The ER stress markers were assessed in cytosolic (GRP-78, eIF2α, p-eIF2α and cleaved caspase-12), nuclear (XBP-1, ATF-4, ATF-6, GADD 153 and cleaved caspase-3) and ER (PERK, pPERK, IRE1α and pIRE1α) fractions of neuro2a cells. The subcellular fractions were prepared according to the method described by Wei-Xing Zong et al. (2003) with slight modifications. Briefly after treatment the cells were scrapped in culture medium and centrifuged at 3000 x rpm for 15 min at 4 °C. The pellet was washed twice with PBS and collected by centrifugation at 3000 x rpm for 10 min at 4 °C. Pellet was suspended in hypotonic buffer A (250 mM sucrose, 20 mM HEPES pH 7.5, 10 mM KCl, 1.5 mM $MgCl_2$, 1 mM EDTA, 1 mM EGTA and 1X protease inhibitor cocktail), kept on ice for 30 min and then cells were disrupted by sonication for 2 min. Cell lysates were centrifuged at 750 × *g* for 10 min at 4 °C to get rid of unlysed cells (supernatant S1) and nuclei (pellet P1). The pellet P1 was resuspended in 100 μl of lysis buffer (250 mM sucrose, 200 mM HEPES pH 7.4, 1 mM DTT, 10 mM KCl, 1.5 mM MgCl2, 1 mM EDTA, 1 mM EGTA, 0.1 mM PMSF and 1X protease inhibitor cocktail) and incubated for 30 min on ice and then centrifuged at 10000 × *g* for 30 min at 4 °C. The supernatant (S2) was saved as the nuclear fraction. The supernatant S1 was centrifuged at 10000 × *g* for 20 min at 4 °C. The pellet (P2) was discarded and then supernatant was centrifuged at 100000 × *g* for 1 h at 4 °C. The supernatant (S3) was saved as the cytosolic fraction. The pellet (P3) was saved as ER fraction. The ER fraction was lysed in RIPA buffer (1% sodium deoxycholine, 0.1% SDS, 1% Triton X-100, 10 mM Tris, pH 8.0, 0.14 M NaCl). The protein content was determined using Lowry's method. Equal amount of protein was loaded in each well in SDS-PAGE and transferred to PVDF membrane. Blocking was done with 5% BSA dissolved in PBS-T. After washing with PBS-T, membranes were incubated with anti GRP-78 (1:500), anti ATF-4 (1:500), anti caspase-12 (1:500), anti eIF2α (1:500), anti peIF2α (1:500), anti GADD 153 (1:500), anti ATF-6 (1:500), anti XBP-1 (1:500), anti caspase-3 (1:500), anti PERK (1:500), anti pPERK (1:500), anti IRE1α (1:500), anti pIRE1α (1:500), anti 3-nitrotyrosine (1:500) and anti β-actin (1:1000) antibodies for overnight. After washing, the membranes were incubated with HRP conjugated secondary antibody (1:2000) for 1–2 h at room temperature. Membranes were washed with PBS-T and developed by chemiluminescence detection using Luminata substrate and signals were captured by chemi doc system XRS + (BioRad). Integrated density of bands was determined and normalized by respective loading control (β-actin for cytosolic fractions, histone for nuclear fractions and calnexin for ER fractions using Image J software.

2.7. Intracellular ROS assay

The levels of intracellular ROS generation were evaluated by dye 2′, 7′-dichlorodihydrofluorescein diacetate (DCFH-DA) as reported previously (Gupta et al., 2014). At the end of treatment the cells were washed with Krebs's ringer (KR) buffer and loaded with DCFH-DA (final concentration 50 μM) for 2 h at 37 °C. Fluorescence was measured by using a fluorimeter (Varian, Cary Eclipse) with excitation at 485 nm and emission at 530 nm.

2.8. Measurement of the nitrite level

Briefly, after treatment the culture medium was collected and incubated with griess reagent containing 0.1% (w/v) napthylethylenediamine HCl and 1% (w/v) sulfanilamide in 5% (v/v) phosphoric acid (vol. 1:1) in the dark for 20 min at room temperature (Esposito et al., 2008). The optical density at 550 nm was measured by using a spectrophotometric microplate reader (Eon, Biotek, USA). Nitrite concentration (in μM) was intrapolated from standard curve of sodium nitrite.

2.9. Measurement of the mitochondrial membrane potential

Mitochondrial membrane potential was estimated by method as described by Hail and Lotan (2000). After treatment the neuro2a cells were stained with rhodamine 123 (10 μg/ml) and incubated in the dark for 1 h at 37 °C. After incubation, the cells were washed with KR buffer and fluorescence intensity was measured by using fluorimeter (Varian Cary Eclipse, USA) at wavelength Ex/Em 508/530 nm.

2.10. Measurements of intracellular calcium

Fluo-3 AM dye was used to measure the intracellular calcium based on protocol described by Xu et al. (2014). At the end of treatment the cells were washed with Krebs's ringer buffer and incubated with Fluo-3 AM (5 μM) for 1 h at 37 °C in dark. After incubation the fluorescence was recorded by flourimeter (Varian, Cary Eclipse) with excitation at

488 nm and emission at 530 nm.

2.11. Hoechst (33342) staining

Condensed nuclei were assessed by a method described by (Watabe and Nakaki., 2004) with some modifications. Briefly, after treatment the cells were washed with PBS and fixed with 4% paraformaldehyde overnight. Fixative was washed with PBS thrice and cells were incubated with Hoechst 33342 dye (1 μg/ml) in the dark at room temperature for 2 h. 40–50 images were captured by using fluorescence microscopy (Nikon, Eclipse TE 2000S and Japan) covering all over area of slide and analyzed.

2.12. Detection of DNA damage

DNA damage was detected by comet assay as previously described (Singh et al., 2011). Briefly, after treatment the cells (1×10^5) were mixed with 200 μl of 0.8% low melting point agarose. The cell suspension was layered on the frosted side of fully frosted slides and kept on ice for solidification of agarose. Then, the slides were kept in lysis buffer for 1 h and then transferred to alkaline buffer for 20 min followed by electrophoresis for 30 min at 15 V and 250 mA. Then, the slides were transferred in 0.4 M tris buffer (pH 7.5) for washing and kept in a humid chamber until staining to prevent it from drying. The staining of slides was done with propidium iodide (40 μg/ml). Sixty to seventy images per slides were captured (microscope, Nikon), and comet parameters: tail length (TL) and olive tail moment (OTM) were analyzed by CASP software.

2.13. Measurements of enzymatic assay for caspase activity

The activity of caspase-3 was measured using the enzyme substrates (Ac-DMQD-AMC) according to manufacturer's protocol. After the desired duration of treatments, the cells were collected as a pellet and resuspended in 1 X lysis buffer and incubated on ice for 20 min. Subsequently, the cells were centrifuged at 10,000 rpm for 10 min at 4 °C and the supernatant was collected and protein was estimated. Then reaction was set up with 50 μg protein was transferred to a 96-well plate to which 200 μl of 1X assay Buffer (20 mM HEPES, pH 7.4, 2 mM EDTA, 0.1% CHAPS, 5 mM DTT) was added. After that, 15 μM of caspase-3 substrate was added and start the reaction by adding 10 μl of caspase −3 substrate. The plate was incubated in the dark for 1 h at 37 °C, and the absorbance was measured at 360excitation/460emmision nm by using florimeter (Eon, Biotek, USA).

2.14. Annexin V-FITC/PI staining

Apoptosis was estimated by using annexin V-FITC/PI staining kit based on the manufacturer's protocol. After treatment, the cells were trypsinized and washed with cold PBS (pH 7.2). The 1×10^6 cells were gently resuspended in 1 X binding buffer and incubated with 1.25 μl of Annexin V-FITC for 15 min in dark. After that, 10 μl of propidium iodide was added and reaction mixture was incubated for 10 min in the dark at room temperature. Fluorescence was measured by flow cytometer (BD FACS Calibur) and analyzed by Cell Quest Pro software (BD).

2.15. Protein estimation

Protein estimation was done in different samples by using Lowry's method (Lowry et al., 1951). The concentration of protein was calculated by standard curve plotted with 1 mg/ml of BSA solution.

2.16. Statistical analysis

Each experiment was performed minimum three times, and the results were presented as the means ± standard error (SEM). Comparison between groups was made by one-way analysis of variance (ANOVA) followed by Newman-Keuls multiple comparisons test. A value of $p < 0.05$ was deemed to be statistically significant.

3. Results

3.1. Selection of salubrinal concentration

The concentration of salubrinal was selected on the basis of cell viability data (Supplementary Fig. 1). Cells were pretreated with salubrinal (5, 10 and 20 μM) for 1 h prior to rotenone (1 μM) treatment. In control cells the MTT reduction was 1.29 ± 0.09 which was significantly ($p < 0.001$) decreased to 0.58 ± 0.06 at 1 μM concentration of rotenone. At the doses of 10 and 20 μM, salubrinal did not offer significant protection against rotenone induced decreased cell viability. However, the 5 μM dose of salubrinal significantly ($p < 0.01$) suppressed the rotenone induced decreased cell viability. The MTT reduction in rotenone (1 μM) + salubrinal (5 μM) treated cells was 0.96 ± 0.11 while the MTT reduction in salubrinal *per se* treated cells was 1.05 ± 0.06 which were both near to control value. Therefore, for further investigation the 5 μM dose of salubrinal was used.

3.2. Salubrinal protects the neuronal cells against rotenone-induced cell death

3.2.1. Cell viability (MTT assay)

Rotenone treatment to neuro2a cells caused significantly ($p < 0.001$) decreased cellular viability at 0.1, 0.5 and 1 μM concentration of rotenone respectively (Fig. 1a). The MTT reduction of control cells was 1.27 ± 0.04 which was significantly decreased to 0.75 ± 0.03, 0.56 ± 0.02 and 0.48 ± 0.02 at 0.1, 0.5 and 1 μM concentration of rotenone respectively. MTT reduction in salubrinal *per se* pretreated cells was 1.15 ± 0.04 reflecting no significant changes in comparison to control cells. Pretreatment of salubrinal (5 μM) offered significant ($p < 0.01$) protection against the rotenone induced decreased MTT reduction. The MTT reduction in rotenone + salubrinal treated cells was 0.89 ± 0.03, 0.71 ± 0.02 and 0.63 ± 0.02 at 0.1, 0.5 and 1 μM concentration of rotenone respectively.

3.2.2. Morphological alterations and cytotoxicity (LDH assay)

Rotenone treatment caused considerably altered morphology of neuro2a cells as well as decreased cell number which was inhibited with pretreatment of salubrinal. Cell lysis was assessed by estimating the lactate dehydrogenase (LDH) activity in cell culture medium. Significant increase in LDH activity was found in culture medium of rotenone treated cells. The LDH activity in culture medium of control cells was 2.78 ± 1.02 per minute/mg of protein which was significantly increased ($p < 0.01$, $p < 0.001$) to 11.61 ± 2.06 and 14.31 ± 2.29 per minute/mg of protein at 0.5 and 1 μM concentration of rotenone respectively. LDH activity in culture medium of salubrinal *per se* pretreated cells was 2.99 ± 1.06 per minute/mg of protein indicating no significant changes in LDH activity in comparison to control cells. Pretreatment of salubrinal (5 μM) offered significant ($p < 0.01$, $p < 0.001$) protection against the rotenone induced increased LDH activity at 0.5 and 1 μM concentration of rotenone. LDH activity in culture medium of rotenone + salubrinal treated cells was 2.68 ± 0.78 and 4.08 ± 1.65 mg of protein per minute at 0.5 and 1 μM concentration of rotenone respectively (Fig. 1b and c).

3.3. Involvement of nitric oxide (NO) mediated ER stress signaling and caspase 3 level

Rotenone treatment to neuro2a cells caused the significantly ($p < 0.001$) increased level of nitrite which was inhibited with aminoguanidine (AG). Since we have observed the significantly increased level of nitrite after rotenone treatment we intend to look into the role

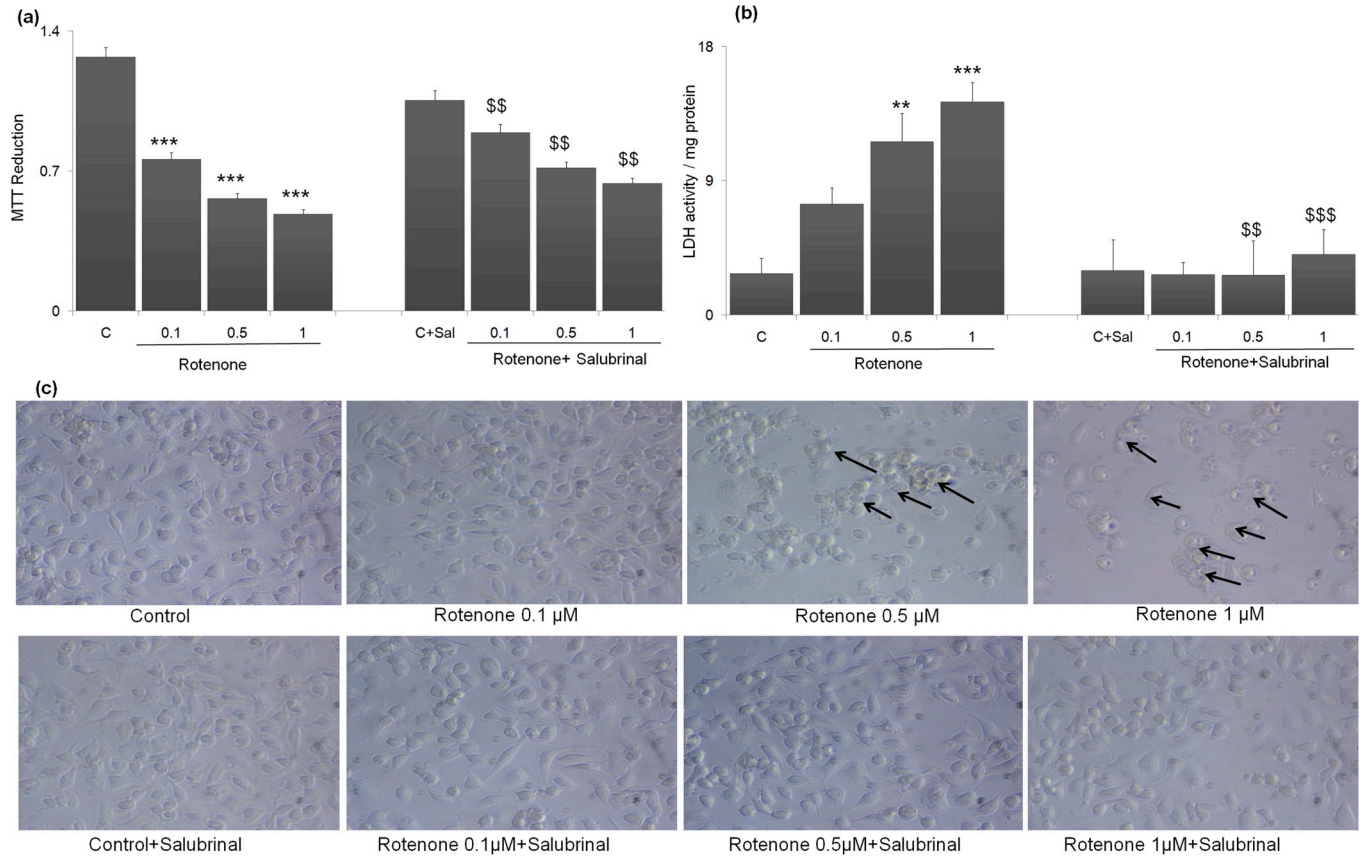

Fig. 1. Cell viability and cytotoxicity. **(a)** Bar diagram represents the effect of rotenone and rotenone + salubrinal on viability of neuro2A cells **(b)** effect of rotenone and rotenone + salubrinal treatment on lactate dehydrogenase (LDH) activity **(c)** Pictorial representation of cellular morphology after treatment of rotenone and rotenone + salubrinal. All the values are in μM. Black arrows indicate the altered morphology of cells. Data are expressed as mean ± SEM and analyzed by ANOVA post hoc Newman-Keuls multiple comparison test. ** = $p < 0.01$, *** = $p < 0.001$ (Control vs. Rotenone treated). $$ = $p < 0.01$, $$$ = $p < 0.001$ (Rotenone treated vs. Rotenone + Salubrinal treated).

of nitric oxide in ER stress related signaling. Therefore the cells were treated with rotenone and/or rotenone + aminoguanidine and the level of key ER stress related markers (GRP78, GADD 153, cleaved caspase-12) and NO production marker (3-nitrotyrosine) was assessed further.

3.3.1. Nitrite level

Nitrite level was significantly ($p < 0.001$) increased in the rotenone treated neuro2a cells (Fig. 2a). The nitrite level in culture medium of control cells was 2.53 ± 0.08 (μM) which was significantly increased to 13.84 ± 4.19 (μM) at highest (1 μM) concentration of rotenone. The nitrite level in culture medium of aminoguanidine *per se* treated cells was 2.14 ± 0.09 (μM) indicating no significant changes in nitrite level in comparison to control cells. Co-treatment of aminoguanidine offered significant ($p < 0.01$) protection against the rotenone induced increased nitrite level and the level in culture medium of rotenone + aminoguanidine co-treated cells was 5.64 ± 0.31 (μM) at 1 μM concentration of rotenone.

3.3.2. Protein abundance of GRP-78, GADD 153, cleaved caspase-12, cleaved caspase-3 and 3-nitrotyosine

Rotenone treatment to neuro2a cells caused significantly increased protein abundance of GRP-78, GADD 153, cleaved caspase-12 and cleaved caspase-3 in comparison to control cells (Fig. 2b). The GRP-78 protein level was significantly ($p < 0.001$) increased in rotenone treated neuro2a cells. The integrated band density of GRP-78 in control cells was 0.77 ± 0.01 which was significantly increased to 1.16 ± 0.04 at highest (1 μM) concentration of rotenone. *Per se* aminoguanidine treatment did not cause alteration in protein abundance of GRP-78 and the integrated band density was 0.73 ± 0.03. Co-treatment of aminoguanidine offered significant ($p < 0.001$) protection against rotenone induced increased level of GRP-78 and the integrated band density in rotenone + aminoguanidine treated cells was 0.91 ± 0.02 at 1 μM concentration of rotenone (Fig. 2c).

The GADD 153 protein abundance was significantly ($p < 0.001$) increased in rotenone treated neuro2a cells. The integrated band density in control cells was 0.66 ± 0.04 which was significantly increased to 1.39 ± 0.06 at 1 μM concentration of rotenone. The integrated band density of GADD 153 in aminoguanidine *per se* treated cells was 0.77 ± 0.03 which is relatively equal to control values revealing that aminoguanidine itself does not have any alteration in protein level of GADD 153. Co-treatment of aminoguanidine significantly ($p < 0.001$) attenuated the rotenone induced increased protein abundance of GADD153. The integrated band density of GADD153 in rotenone + aminoguanidine treated neuro2a cells was 0.48 ± 0.03 at 1 μM concentration of rotenone (Fig. 2d).

Cleaved caspase-12 protein abundance was also significantly ($p < 0.001$) increased in neuro2a cells after rotenone treatment. The integrated band density of cleaved caspase-12 in control cells was 0.13 ± 0.003 which was significantly increased to 0.95 ± 0.01 at 1 μM concentration of rotenone. In *per se* aminoguanidine treated cells the integrated band density was 0.26 ± 0.009 reflecting no effect of aminoguanidine itself on cleaved caspase-12 protein level. Co-treatment of aminoguanidine significantly ($p < 0.001$) inhibited the protein level of cleaved caspase-12 and the integrated band density in rotenone + aminoguanidine treated cells was 0.33 ± 0.008 at 1 μM concentration of rotenone (Fig. 2e).

The rotenone treatment to neuro2a cells also caused significantly increased ($p < 0.001$) protein abundance of cleaved caspase-3. The

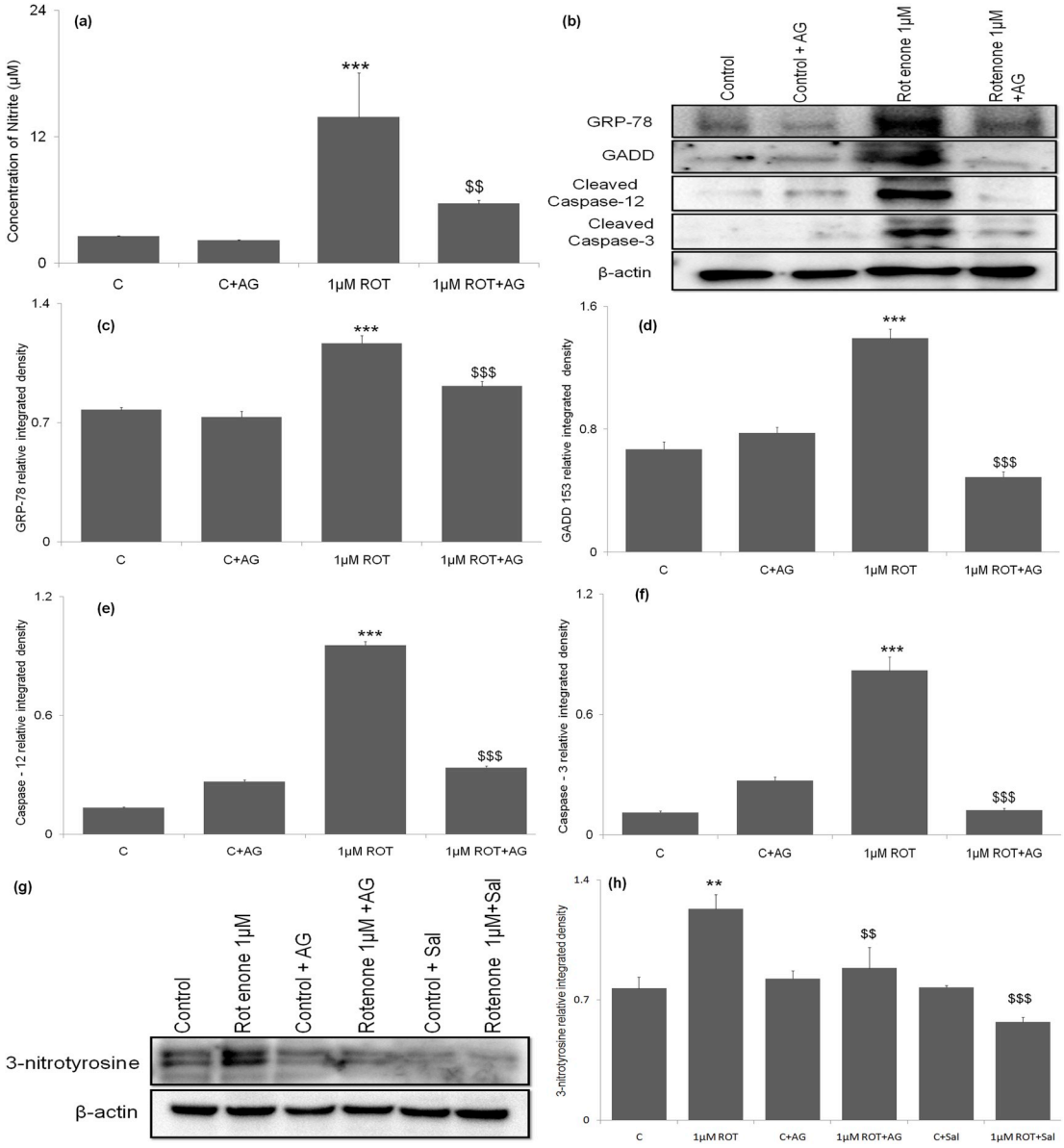

Fig. 2. Nitric oxide mediated ER stress signaling. **(a)** Graphical representation of nitrite level after 24 h of rotenone + aminoguanidine (AG) treatment in neuro2A cells. **(b)** Images representing the protein abundance of GRP-78, GADD 153,Caspase-12, Caspase-3 along with β-actin as loading control after 24 h of rotenone and rotenone + aminoguanidine (AG) treatment in neuro2A cells. **(c–f)** Bar diagram representing the quantification of observed protein level with respect to loading control β-actin. **(g)** Image represents the protein abundance of 3-nitrotyrosine after 24 h of different treatment. **(h)** Bar diagram represents the quantification of nitrotyrosine abundance with respect to loading control β-actin. Data are expressed as mean ± SEM, analyzed by ANOVA post hoc Newman-Keuls multiple comparison test. ** = $p < 0.01$, *** = $p < 0.001$ (Control vs. Rotenone treated). $$ = $p < 0.01$, $$$ = $p < 0.001$ (Rotenone treated vs. Rotenone + Aminoguanidine treated).

integrated band density of cleaved caspase-3 in control cells was 0.11 ± 0.008 which was significantly increased to 0.81 ± 0.06 at 1 μM concentration of rotenone. The integrated band density in aminoguanidine *per se* treated cells was 0.27 ± 0.01, indicating no significant changes in cleaved caspase-3 level in comparison to control cells. Co-treatment of aminoguanidine offered significant ($p < 0.001$) protection against rotenone induced increased protein level of cleaved caspase-3. The integrated band density of cleaved caspase-3 in rotenone + aminoguanidine treated cells was 0.12 ± 0.01 at 1 μM concentration of rotenone (Fig. 2f).

Protein abundance of 3-nitrotyosine was significantly ($p < 0.01$) increased in neuro2a cells after rotenone treatment (Fig. 2g). The integrated band density of 3-nitrotyosine in control cells was 0.768 ± 0.06 which was significantly increased 1.23 ± 0.08 at highest concentration (1 μM) of rotenone. *Per se* treatment of aminoguanidine and/or salubrinal to cells showed the integrated band density of 0.82 ± 0.04 and 0.77 ± 0.01 respectively reflecting no effect of aminoguanidine and salubrinal itself on 3-nitrotyosine protein level. Co-treatment of aminoguanidine with rotenone significantly ($p < 0.01$) inhibited the rotenone induced augmented protein level of 3-nitrotyosine and the integrated band density in rotenone (1 μM) + aminoguanidine treated cells was 0.88 ± 0.12 at 1 μM concentration of rotenone. Pretreatment of salubrinal (5 μM) also offered significant ($p < 0.001$) protection against the rotenone induced increased protein level of 3-nitrotyosine at 1 μM concentration of rotenone. Integrated band intensity of 3-nitrotyosine in rotenone + salubrinal treated cells was 0.57 ± 0.02 at 1 μM concentration of rotenone (Fig. 2h).

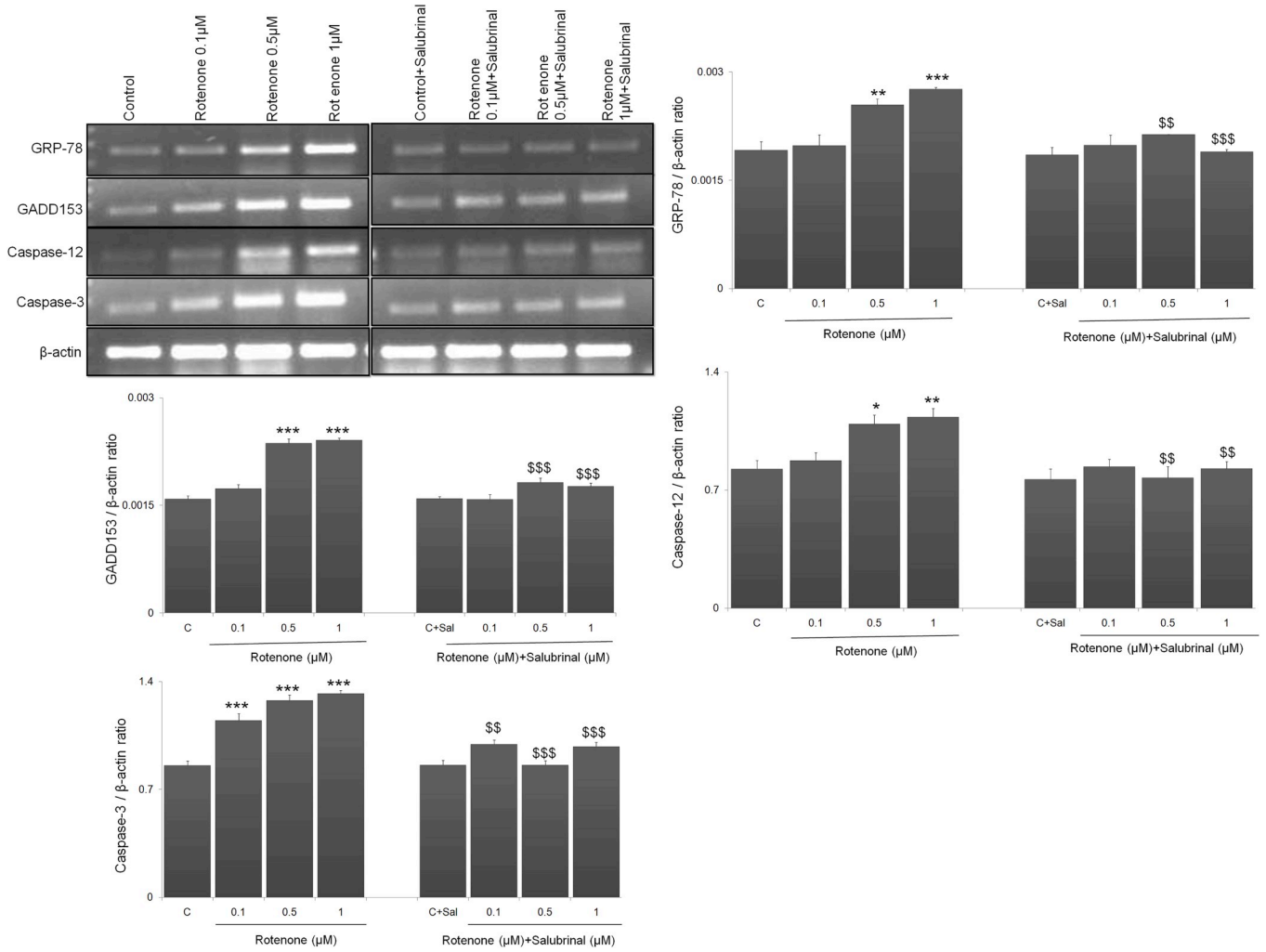

Fig. 3. mRNA levels of various factors. Images representing the mRNA levels of key factors of endoplasmic reticulum stress signaling after 24 h of rotenone and rotenone + salubrinal treatment in neuro2A cells. Bar diagram representing the quantification of observed mRNA level with respect to loading control β-actin. Data are expressed as mean ± SEM, analyzed by ANOVA post hoc Newman-Keuls multiple comparison test. * = $p < 0.05$, ** = $p < 0.01$, *** = $p < 0.001$ (Control vs. Rotenone treated). $$ = $p < 0.01$, $$$ = $p < 0.001$ (Rotenone treated vs. Rotenone + Salubrinal treated).

3.4. Salubrinal inhibits the mRNA level of ER stress key markers (GRP-78, GADD 153, caspase-12 and caspase-3)

The neuro2a cells were treated with different concentration of rotenone (0.1, 0.5 and 1 μM) for 24 h. Rotenone caused significantly ($p < 0.001$) increased mRNA level of GRP-78, GADD 153, caspase-12 and caspase-3 in a dose-dependent manner (Fig. 3) in comparison to control cells. Pretreatment of salubrinal offered significant ($p < 0.001$) protection against rotenone induced increased mRNA level of GRP-78, GADD 153, caspase-12 and caspase-3.

Rotenone treatment to neuro2a cells caused significantly increased mRNA level of GRP-78 in comparison to control cells. The integrated band density of GRP-78 in control cells was 1.9 ± 0.1 which was significantly ($p < 0.01$, $p < 0.001$) increased to 2.5 ± 0.1 and 2.7 ± 0.3 at 0.5 and 1 μM concentration of rotenone respectively. *Per se* treatment of salubrinal did not cause alteration in mRNA level of GRP-78 in comparison to control cells and the integrated band density in salubrinal *per se* pretreated cells was 1.8 ± 0.1. Pretreatment of salubrinal offered significant ($p < 0.01$, $p < 0.001$) protection against rotenone induced increased mRNA level of GRP-78. The integrated band density in rotenone + salubrinal treated cells was 2.1 ± 0.1 and 1.8 ± 0.2 at 0.5 and 1 μM concentration of rotenone respectively.

Similarly, mRNA level of GADD153 was significantly increased after rotenone treatment to neuro2a cells as compared to control cells. The integrated band density of GADD153 in control cells was 1.5 ± 0.3 which was significantly ($p < 0.001$) increased to 2.3 ± 0.2 and 2.4 ± 0.5 at 0.5 and 1 μM concentration of rotenone respectively. *Per se* treatment of salubrinal did not cause alteration in mRNA level of GADD153 in comparison to control cells and the integrated band density in salubrinal *per se* pretreated cells was 1.5 ± 0.5. Pretreatment of salubrinal offered significant ($p < 0.001$) protection against rotenone induced increased mRNA level of GADD153. The integrated band density in rotenone + salubrinal treated cells was 1.8 ± 0.6 and 1.7 ± 0.4 at 0.5 and 1 μM concentration of rotenone respectively.

The mRNA level of caspase-12 was also significantly augmented in rotenone treated neuro2a cells. The integrated band density of caspase-12 in control cells was 0.825 ± 0.049 which was significantly ($p < 0.05$, $p < 0.01$) increased to 1.09 ± 0.06 and 1.13 ± 0.06 at 0.5 and 1 μM concentration of rotenone respectively. *Per se* treatment of salubrinal indicated no alteration in mRNA level of caspase-12 and the integrated band density in salubrinal *per se* pretreated cells was 0.765 ± 0.046. Pretreatment of salubrinal significantly ($p < 0.01$) attenuated the rotenone induced increased mRNA level of caspase-12. The integrated band density in rotenone + salubrinal treated cells was 0.77 ± 0.04 and 0.82 ± 0.04 at 0.5 and 1 μM concentration of rotenone respectively.

Rotenone treatment to neuro2a cells for 24 h caused significantly

increased mRNA level of caspase-3 in comparison to control cells. The integrated band density of caspase-3 in control cells was 0.857 ± 0.026 which was significantly ($p < 0.001$) increased to 1.14 ± 0.03, 1.27 ± 0.02 and 1.32 ± 0.02 at 0.1, 0.5 and 1 μM concentration of rotenone respectively. *Per se* salubrinal treatment indicated no alteration in mRNA level of caspase-3 and the integrated band density in salubrinal *per se* pretreated cells was 0.859 ± 0.042. Pretreatment of salubrinal significantly ($p < 0.001$) attenuated the rotenone induced increased mRNA level of caspase-3. The integrated band density in rotenone + salubrinal treated cells was 0.99 ± 0.01, 0.85 ± 0.02 and 0.97 ± 0.02 at 0.1, 0.5 and 1 μM concentration of rotenone respectively.

3.5. Salubrinal protects against rotenone-induced ER stress mediated signaling

Since we have observed the salubrinal induced significant attenuation against rotenone induced augmented level of key ER Stress related transmembrane kinases and chaperon. Further we intend to investigate the effect of salubrinal on the subsequent signaling mechanism to entirely understand the probable therapeutic effect of salubrinal in ER stress related neuronal death mechanisms and diseases. Since we have already observed the augmented level of nitrite/NOS, which is critical in ER stress related pathways (Gupta et al., 2015a,b: koji takadaet al., 2013: Dickhout et al., 2005) and we have observed the aminoguanidine (NOS inhibitor) induced inhibition in ER stress marker therefore further investigation was done to evaluate the effect of salubrinal on other ER stress related signaling and explore its neuroprotective activity. Since ER stress initiates after dissociation of GRP78 and subsequent activation of transmembrane kinases (PERK & IRE1α/pIRE1α) and ATF6 (Walter and Ron, 2011; Rutkowski and Hegde, 2010) therefore effect of said kinases mediated signaling factor was assessed (Fig. 4a). The protein expression of all ER stress signaling factors was significantly increased along with dephosphorylation of eIF2α. Salubrinal pretreatment significantly attenuated the rotenone induced altered expression of all ER stress signaling markers and cleaved caspase-3 as given in details below (Fig. 4b). However, the levels of PERK and IRE1α remain unaltered after rotenone treatment.

3.5.1. GRP-78

GRP-78 protein abundance was significantly ($p < 0.001$) increased after rotenone treatment in neuro2a cells. The integrated band density of GRP-78 in control cells was 0.09 ± 0.02 which was significantly increased to 0.38 ± 0.06 and 0.43 ± 0.09 at 0.5 and 1 μM concentration of rotenone respectively. The integrated band density in *per se* salubrinal treated cells was 0.08 ± 0.006 reflecting no effect of salubrinal itself on GRP78 protein level. Pretreatment of salubrinal offered significant ($p < 0.001$) protection against rotenone induced increased protein abundance of GRP-78. The integrated band density of rotenone + salubrinal treated cells was 0.13 ± 0.01 and 0.03 ± 0.004 at 0.5 and 1 μM concentration of rotenone respectively.

3.5.2. pPERK

The rotenone treatment to neuro2a cells caused significantly increased phosphorylation of PERK protein. The integrated band density of pPERK in control cells was 0.39 ± 0.03 which was significantly ($p < 0.001$) increased to 0.67 ± 0.03 at 1 μM concentration of rotenone. *Per se* salubrinal treatment did not cause alteration in protein abundance of pPERK and the integrated band density was 0.39 ± 0.03. Pretreatment of salubrinal offered significant ($p < 0.001$) attenuation against rotenone induced increased phophorylation of PERK. The integrated band density of rotenone + salubrinal treated neuro2a cells was 0.30 ± 0.02 at 1 μM concentration of rotenone respectively.

3.5.3. p-eIF2α

Protein abundance of p-eIF2α was significantly ($p < 0.001$) decreased in rotenone treated neuro2a cells. In control cells the integrated band density was 1.03 ± 0.03 while in *per se* salubrinal treated cells the integrated band density was 1.15 ± 0.04. The integrated band density of p-eIF2α was significantly decreased to 0.37 ± 0.03 and 0.62 ± 0.04 at 0.5 and 1 μM concentration of rotenone respectively as compared to control cells. Pretreatment of salubrinal offered significant ($p < 0.001$) protection against rotenone induced decreased protein abundance of p-eIF2α. The band integrated density of rotenone + salubrinal treated cells was 0.83 ± 0.04 and 0.62 ± 0.04 at 0.5 and 1 μM concentration of rotenone respectively.

3.5.4. ATF-4

The ATF-4 protein abundance was also significantly ($p < 0.05$) increased in rotenone treated neuro2a cells. The integrated band density of ATF-4 in control cells was 0.06 ± 0.02 which was significantly increased to 0.14 ± 0.02 and 0.15 ± 0.02 at 0.5 and 1 μM concentration of rotenone respectively. The integrated band density of ATF-4 in salubrinal *per se* pretreated cells was 0.08 ± 0.004 which was near to control value. Pretreatment of salubrinal significantly ($p < 0.05$) decreased the protein abundance of ATF-4 and the integrated band density in rotenone + salubrinal treated cells was 0.05 ± 0.001 and 0.06 ± 0.007 at 0.5 and 1 μM concentration of rotenone respectively.

3.5.5. pIRE1α

The rotenone treatment to neuro2a cells caused significantly increased ($p < 0.001$) phosphorylation of IRE1α protein. In control cells the integrated band density of pIRE1α was 0.29 ± 0.02 which was significantly increased to 0.479 ± 0.025, 0.582 ± 0.050 and 0.694 ± 0.060 at 0.1, 0.5 and 1 μM concentration of rotenone respectively. *Per se* treatment of salubrinal did not cause alteration in protein abundance of pIRE1α and the integrated band density was 0.27 ± 0.01. Pretreatment of salubrinal offered significant ($p < 0.01$) attenuation against rotenone induced increased protein abundance of pIRE1α. The integrated band density in rotenone + salubrinal treated neuro2a cells was 0.41 ± 0.01 and 0.46 ± 0.03 at 0.5 and 1 μM concentration of rotenone respectively.

3.5.6. XBP-1

Protein abundance of XBP-1 was also significantly increased ($p < 0.001$) in neuro2a cells after rotenone treatment. In control cells the integrated band density of XBP-1 was 0.07 ± 0.01 which was significantly increased to 0.16 ± 0.007, 0.18 ± 0.009 and 0.26 ± 0.008 at 0.1, 0.5 and 1 μM concentration of rotenone respectively. The integrated band density of XBP-1in salubrinal *per se* pretreated cells was 0.07 ± 0.002 which is relatively equal to control value. Pretreatment of salubrinal offered significant (($p < 0.05$, $p < 0.001$) protection against rotenone induced increased protein abundance of XBP-1. The integrated band density in rotenone + salubrinal treated cells was 0.11 ± 0.016 and 0.17 ± 0.017 at 0.5 and 1 μM concentration of rotenone respectively.

3.5.7. ATF-6

The rotenone treatment to neuro2a cells caused significantly increased ($p < 0.001$) protein abundance of ATF-6. The integrated band density of ATF-6 in control cells was 0.13 ± 0.003 which was significantly increased to 0.33 ± 0.006, 0.36 ± 0.01 and 0.42 ± 0.02 at 0.1, 0.5 and 1 μM concentration of rotenone respectively. The integrated band density in *per se* salubrinal pretreated cells was 0.14 ± 0.005 reflecting no effect of salubrinal itself on ATF-6 protein level. Pretreatment of salubrinal provided significant ($p < 0.01$) protection against rotenone induced increased protein abundance of ATF-6. The integrated band density of ATF-6 in rotenone + salubrinal treated cells was 0.11 ± 0.004 and 0.13 ± 0.004 at 0.5 and 1 μM concentration of rotenone respectively.

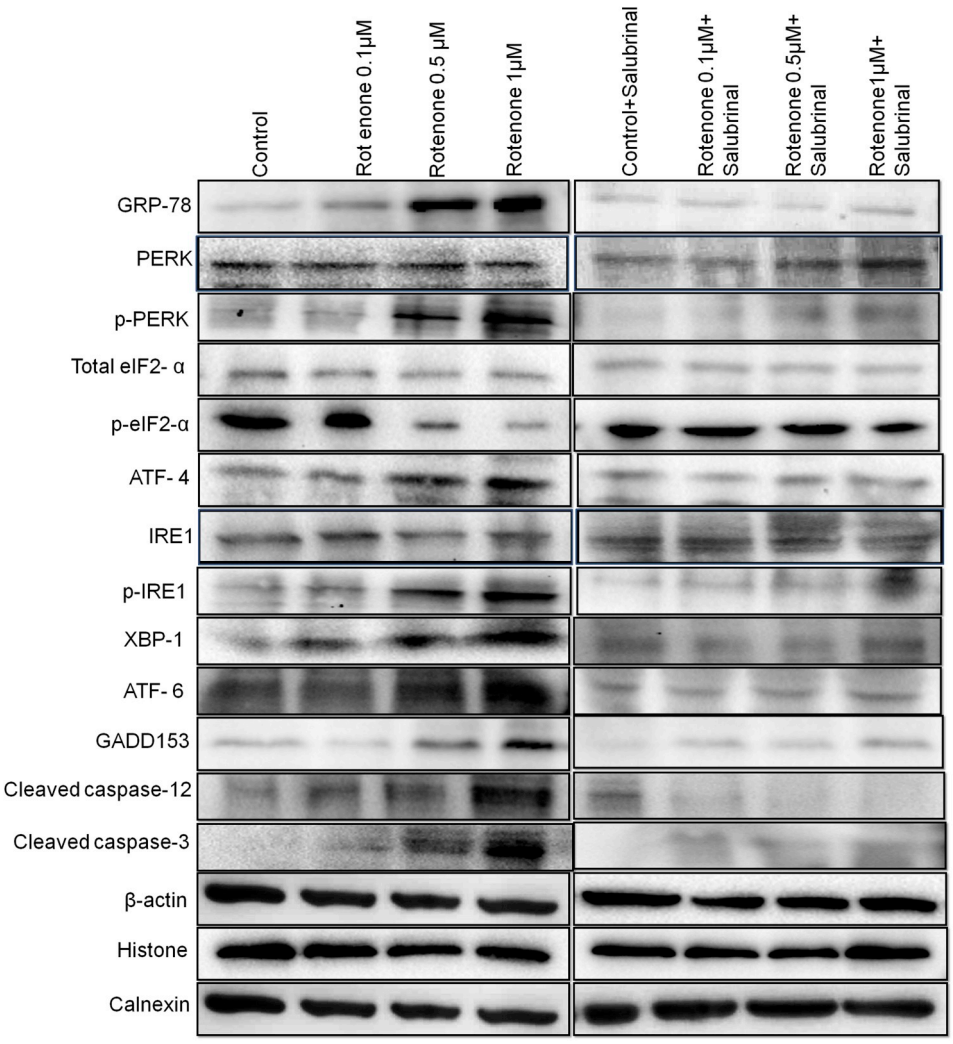

Fig. 4a. Blots showing the levels of various factors. Images showing the protein abundance of endoplasmic reticulum (ER) stress signaling markers GRP-78, p-PERK, eIF2-α, p-eIF2-α, IRE1α, p-IRE1α, ATF-4, XBP-1, ATF-6, GADD153, cleaved caspase-12, cleaved caspase-3 along with β-actin, histone, calnexin as loading control after 24 h of rotenone and rotenone + salubrinal treatment in neuro2A cells. IRE1α, p-IRE1α, PERK, p-PERK were estimated in ER fraction. GRP-78, eIF2-α, p-eIF2-α, caspase-12 were estimated in cytosolic fraction while caspase-3, GADD 153, XBP-1, ATF-4 and ATF-6 were estimated in nuclear fraction.

3.5.8. GADD 153

The GADD 153 protein abundance was significantly ($p < 0.01$, $p < 0.001$) increased to 2.18 ± 0.04 and 2.41 ± 0.11 at 0.5 and 1 μM concentration of rotenone respectively as compared to control cells. The integrated band density in control cells was 1.43 ± 0.01. The integrated band density of GADD 153 in salubrinal *per se* pretreated cells was 1.47 ± 0.14 which is relatively equal to control value. Pretreatment of salubrinal offered significant ($p < 0.01$, $p < 0.001$) protection against rotenone induced increased protein abundance of GADD153. The integrated band density of GADD153 in rotenone + salubrinal treated neuro2a cells was 1.5 ± 0.14 and 1.53 ± 0.15 at 0.5 and 1 μM concentration of rotenone respectively.

3.6. Cleaved caspase-12

ER specific cleaved caspase-12 protein abundance was significantly increased in neuro2a cells after rotenone treatment. The integrated band density of cleaved caspase-12 in control cells was 0.90 ± 0.06 which was significantly ($p < 0.01$, $p < 0.001$) increased to 1.631 ± 0.141 and 1.852 ± 0.205 at 0.5 and 1 μM concentration of rotenone respectively. The integrated band density in *per se* salubrinal pretreated cells was 0.96 ± 0.07 reflecting no effect of salubrinal itself on cleaved caspase-12 protein level. Pretreatment of salubrinal significantly ($p < 0.001$) decreased the protein abundance of cleaved caspase-12 and the integrated band density in rotenone + salubrinal treated cells was 0.78 ± 0.05 and 0.44 ± 0.04 at 0.5 and 1 μM concentration of rotenone respectively.

3.6.1. Cleaved caspase-3

The rotenone treatment to neuro2a cells caused significantly increased ($p < 0.001$) protein abundance of cleaved caspase-3. The integrated band density of cleaved caspase-3 in control cells was 0.15 ± 0.01 which was significantly increased to 0.30 ± 0.02, 0.36 ± 0.02 and 0.43 ± 0.03 at 0.1, 0.5 and 1 μM concentration of rotenone respectively. The integrated band density in salubrinal *per se* pretreated cells was 0.19 ± 0.01, indicating no significant changes in protein abundance of cleaved caspase-3 in comparison to control cells. Pretreatment of salubrinal offered significant ($p < 0.001$) protection against only at highest concentration of rotenone. The integrated band density of cleaved caspase-3 in rotenone + salubrinal treated cells was 0.21 ± 0.01 at 1 μM concentration of rotenone.

Salubrinal attenuates rotenone induced altered intracellular ROS level, MMP level, Nitrite level and intracellular calcium level.

3.6.2. Reactive oxygen species (ROS)

Reactive oxygen species (ROS) like superoxide and hydrogen

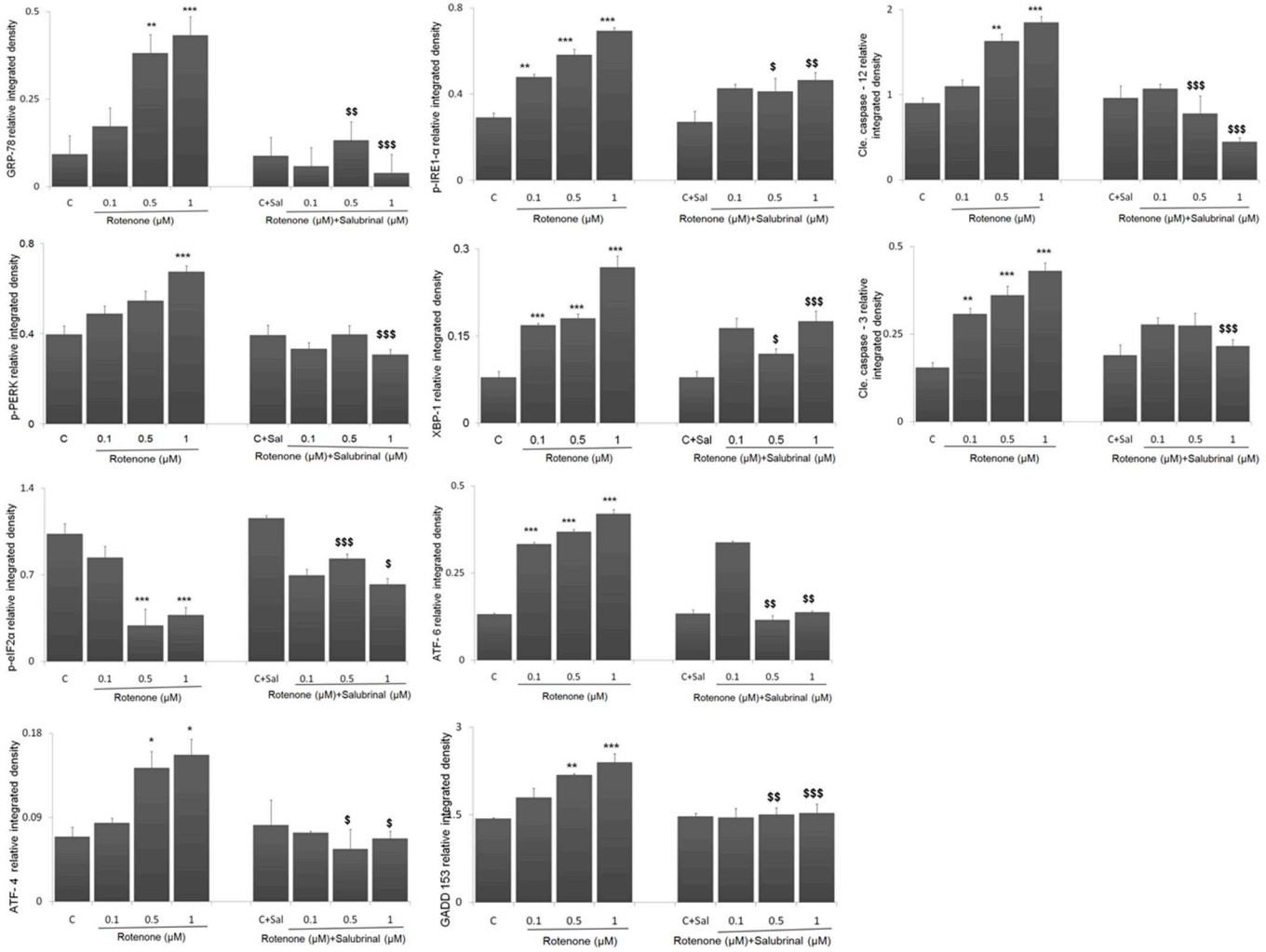

Fig. 4b. Quatitative representation of protein levels of various factors. Graphical representation illustrating quantification of various proteins abundance with the loading control β-actin; in cytosolic fractions (GRP-78, eIF2-α, p-eIF2-α, caspase-12), nuclear fractions (XBP-1, ATF-4, ATF-6, GADD153, caspase-3) and endoplasmic reticulum fractions (pIRE-1α, p-PERK). Data are expressed as mean ± SEM, analyzed by ANOVA post hoc Newman-Keuls multiple comparison test. * = $p < 0.05$,** = $p < 0.01$,*** = $p < 0.001$ (Control vs. Rotenone treated). $ = $p < 0.05$, $$ = $p < 0.01$, $$$ = $p < 0.001$ (Rotenone treated vs. Rotenone + Salubrinal treated).

peroxide are continually produced during cellular metabolic processes. The level of ROS was estimated by using (DCFH-DA). Rotenone treatment to neuro2a cells caused significantly ($p < 0.001$) increased ROS level at 1 μM concentration of rotenone (Fig. 5a). In control cells the fluorescence intensity (a.u) was 11.61 ± 0.46 whereas the fluorescence intensity (a.u) of rotenone treated cells was 14.55 ± 0.52, 16.67 ± 0.50 and 18.70 ± 0.72 at 0.1, 0.5 and 1 μM concentration of rotenone respectively. Fluorescence intensity (a.u) in salubrinal *per se* pretreated cells was 12.13 ± 0.49 which was not significantly different than the observed ROS level in control cells. Pretreatment of salubrinal significantly ($p < 0.001$) decreased the rotenone induced ROS generation at 1 μM concentration of rotenone. The fluorescence intensity (a.u) in rotenone + salubrinal treated cells was 14.35 ± 0.54 at 1 μM concentration of rotenone respectively.

3.6.3. Mitochondrial membrane potential (MMP)

Rhodamine 123 was used to monitor the membrane potential of mitochondria. Rotenone treatment to neuro2a cells caused significantly ($p < 0.001$) decreased MMP level (Fig. 5b). In control cells the fluorescence intensity (a.u) was 47.04 ± 4.18 which was significantly diminished to 31.91 ± 2.05, 28.54 ± 1.94 and 23.69 ± 1.10 at 0.1, 0.5 and 1 μM concentration of rotenone respectively. Fluorescence intensity (a.u) in salubrinal *per se* pretreated cells was 47.37 ± 3.90 which is relatively equal to control values revealing that salubrinal itself does not have any alteration in MMP level. Pretreatment of salubrinal significantly ($p < 0.01$) inhibited the rotenone induced decreased MMP level. The fluorescence intensity (a.u) in rotenone + salubrinal treated cells was 43.84 ± 3.26, 41.45 ± 2.83 and 36.74 ± 2.55 at 0.1, 0.5 and 1 μM concentration of rotenone respectively.

3.6.4. Nitrite level

Rotenone treatment to neuro2a cells caused significantly increased nitrite level at 1 μM concentration of rotenone (Fig. 5c). The nitrite level in culture medium of control cells was 10.86 ± 1.41 (μM) which was significantly ($p < 0.001$) increased to 25.47 ± 2.90 (μM) at 1 μM concentration of rotenone. The nitrite level in culture medium of salubrinal *per se* pretreated cells was 10.71 ± 2.09 (μM) which is comparable to control cells. Pretreatment of salubrinal offered significant ($p < 0.001$) protection against the rotenone induced nitrite level at 1 μM concentration of rotenone. Nitrite level in culture medium of rotenone + salubrinal treated cells was 6.81 ± 0.94 (μM) at 1 μM concentration of rotenone respectively.

3.6.5. Intracellular calcium

Fluo-3 AM is a cell-permeable fluorescent calcium indicator,

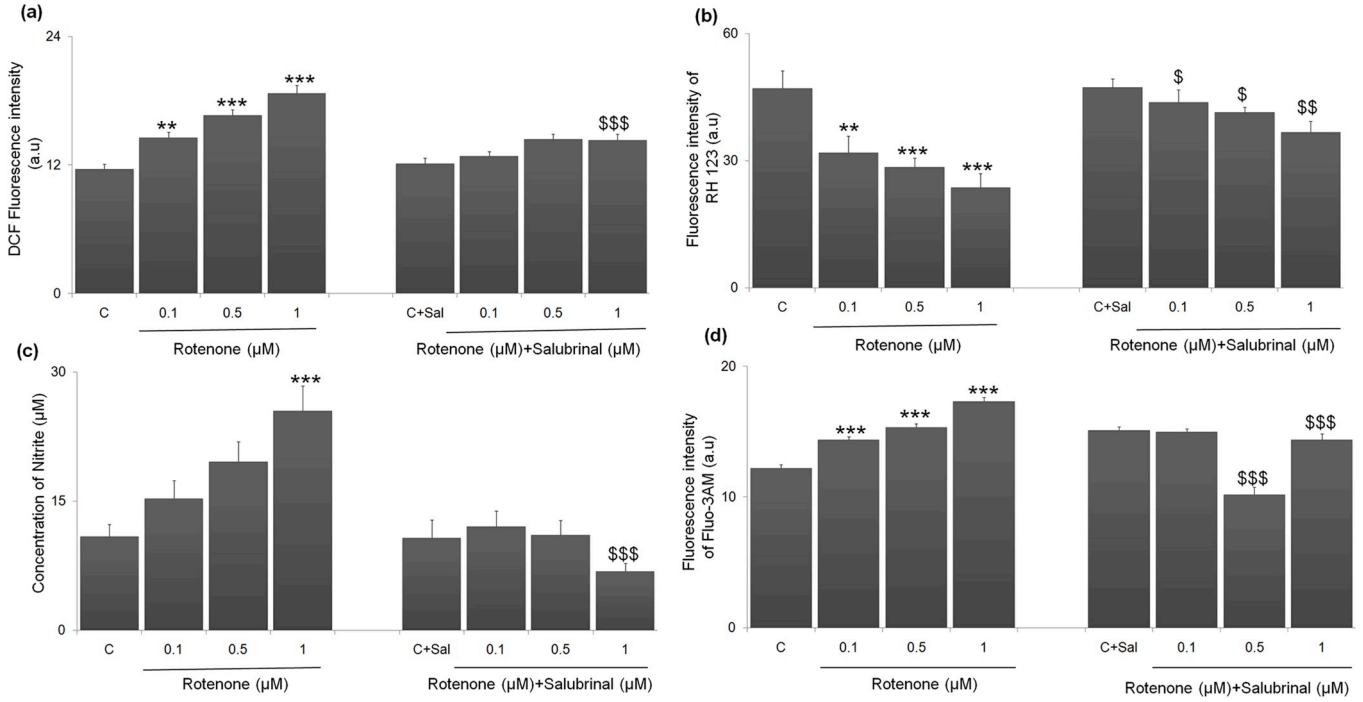

Fig. 5. Biochemical alterations in cells. Graphical representation of **(a)** ROS generation, **(b)** mitochondrial membrane potential (rhodamine 123 fluorescence), **(c)** nitrite level and **(d)** intracellular calcium level after 24 h of rotenone and rotenone + salubrinal treatment in neuro2A cells. Data are expressed as mean ± SEM, analyzed by ANOVA post hoc Newman-Keuls multiple comparison test. ** = $p < 0.01$, *** = $p < 0.001$ (Control vs. Rotenone treated). $ = $p < 0.05$, $ $ = $p < 0.01$, $$$ = $p < 0.001$ (Rotenone treated vs. Rotenone + Salubrinal treated).

commonly used in cell-based experiments to detect changes in intracellular calcium levels. Rotenone treatment to neuro2a cells showed significantly ($p < 0.001$) elevated intracellular calcium level (Fig. 5d). The fluorescence intensity (a.u) in control neuro2a cells was 12.21 ± 0.26 whereas the fluorescence intensity (a.u) of rotenone treated cells was 14.38 ± 0.26, 15.35 ± 0.29 and 17.32 ± 0.59 at 0.1, 0.5 and 1 μM concentration of rotenone respectively. Fluorescence intensity (a.u) in salubrinal *per se* pretreated cells was 15.11 ± 0.23 which was near to control value. Pretreatment of salubrinal significantly ($p < 0.001$) decreased the rotenone induced increased intracellular calcium level. The fluorescence intensity (a.u) in rotenone + salubrinal treated cells was 14.99 ± 0.29, 10.19 ± 0.23 and 14.38 ± 0.46 at 0.1, 0.5 and 1 μM concentration of rotenone respectively.

3.7. Salubrinal inhibits the rotenone-induced neuronal cell death

3.7.1. Chromatin condensation

Hoechst 33342 is a widespread cell-permeable nuclear counter stain that emits the blue fluorescence when bound to dsDNA. This dye is being used to distinguish condensed pyknotic nuclei in apoptotic cells. Hoechst staining revealed that rotenone treatment to neuro2a cells caused significant ($p < 0.001$) increase in the number of condensed nuclei (Fig. 6a). In control cells the ratio of condensed nuclei was 21.45 ± 3.90 which was significantly increase to 57.65 ± 4.00, 64.43 ± 3.64 and 71.31 ± 3.87 at 0.1, 0.5 and 1 μM concentration of rotenone respectively. The ratio of condensed nuclei in salubrinal *per se* pretreated cells was 25.43 ± 1.98, indicating no significant changes in condensed nuclei in comparison to control cells. Pretreatment of salubrinal significantly ($p < 0.001$) decreased the ratio of condensed nuclei. The ratio of condensed nuclei in rotenone + salubrinal treated cells was 44.62 ± 3.00, 45.02 ± 2.37, and 47.51 ± 3.60 at 0.1, 0.5 and 1 μM concentration of rotenone respectively.

3.7.2. DNA damage

Rotenone treatment to neuro2a cells caused significantly ($p < 0.001$) increased DNA damage as observed by comet assay by estimating two parameters tail length (TL) and olive tail moment (OTM). In control cells the OTM and TL was 3.02 ± 0.10 (a.u) and 28.14 ± 0.61 (a.u) respectively (Fig. 6b). Rotenone treatment to neuro2a cells caused the DNA strand breaks and the OTM was 26.41 ± 1.20 (a.u) and 26.80 ± 1.29 (a.u) at 0.5 and 1 μM concentration of rotenone respectively. The TL in rotenone treated cells was 83.37 ± 2.31 (a.u) and 83.93 ± 2.18 (a.u) at 0.5 and 1 μM concentration of rotenone respectively. In salubrinal *per se* pretreated cells, OTM and TL was 3.89 ± 0.13 (a.u) and 23.84 ± 0.49 (a.u) respectively indicating no significant changes in DNA damage in comparison to control cells. Pretreatment of salubrinal significantly ($p < 0.01$) decreased the rotenone induced DNA damage. The OTM in rotenone + salubrinal treated cells was 7.04 ± 0.39 (a.u) and 7.28 ± 0.50 (a.u) at 0.5 and 1 μM concentration of rotenone respectively. The TL in rotenone + salubrinal treated cells was 35.62 ± 1.02 and 33.38 ± 1.14 (a.u) at 0.5 and 1 μM concentration of rotenone respectively.

3.7.3. Caspase-3 activity

Detection of caspase-3 activity provides the details regarding one of the earliest known biochemical events associated with apoptosis (Figure 6c). Caspase-3 activity was significantly ($p < 0.001$) increased in neuro2a cells after rotenone treatment. Caspase-3 activity in control cells was 34.03 ± 1.47 which was significantly increased to 42.33 ± 0.40 at highest concentration (1 μM) of rotenone. In *per se* aminoguanidine and salubrinal treated cells the caspase-3 activity was 37.82 ± 0.63 and 37.87 ± 0.92 respectively indicating no effect of aminoguanidine and salubrinal on caspase-3 activity. Co-treatment of rotenone with aminoguanidine significantly ($p < 0.001$) inhibited the caspase-3 activity and the level in rotenone + aminoguanidine treated cells was 35.35 ± 1.83 at 1 μM concentration of rotenone. Pretreatment of salubrinal (5 μM) also offered significant ($p < 0.001$)

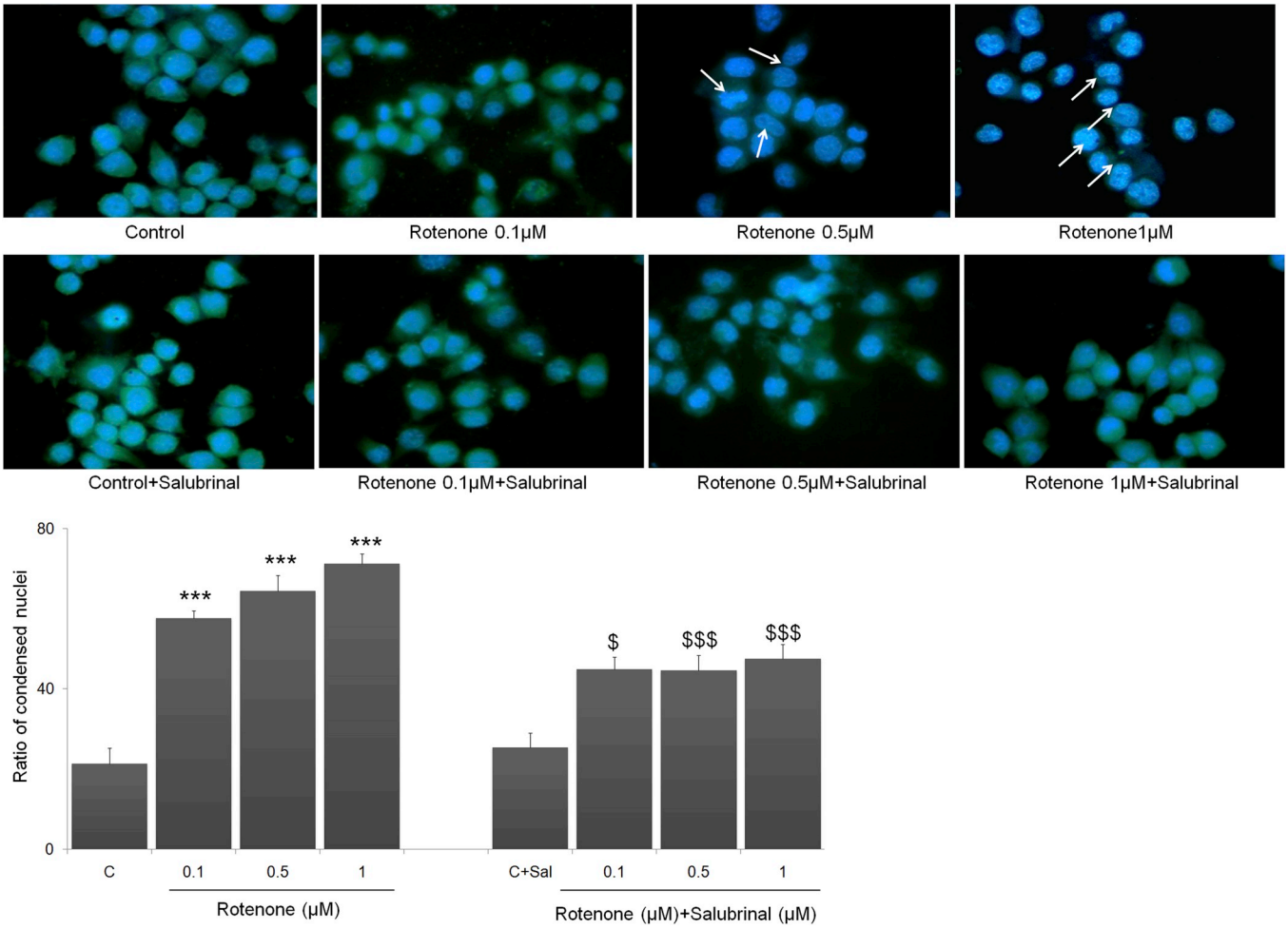

Fig. 6a. Hoechst stainning in cells. Images showing alteration in nuclear morphology after rotenone and rotenone + salubrinal treatment in neuro2A cells. Arrows indicate the alterations in nuclear morphology. Bar diagram represents the ratio of condensed nuclei (condensed/total nuclei). Data are expressed as mean ± SEM, analyzed by ANOVA post hoc Newman-Keuls multiple comparison test. *** = $p < 0.001$ (Control vs. Rotenone treated). $ = $p < 0.05$, $$$ = $p < 0.001$ (Rotenone treated vs. Rotenone + Salubrinal treated).

protection against the rotenone induced increased caspase-3 activity at 1 μM concentration of rotenone and the caspase-3 activity was 37.42 ± 0.88.

3.7.4. Annexin V-FITC/PI staining by flow cytometry

The apoptotic death of cells was assessed by staining the cells with annexin V-FITC and PI and analyzed by FACS. The quantitation determines the percentage of early and late apoptotic cells (Fig. 6d). In control cells the percentage of early and late apoptotic cells was 4.22 ± 0.59 percent and 3.49 ± 0.08 percent respectively which was significantly ($p < 0.001$, $p < 0.01$) increased to 9.66 ± 1.40 percent and 14.31 ± 1.66 percent at 1 μM concentration of rotenone respectively. In salubrinal *per se* pretreated cells the percentage of early and late apoptotic cells was 3.28 ± 0.28 percent and 4.97 ± 1.31 percent respectively indicating no significant changes in apoptotic cells in comparison to control cells. Pretreatment of salubrinal significantly ($p < 0.001$, $p < 0.01$) decreased the rotenone induced apoptotic death of cells. The percentage of early and late apoptotic cells in rotenone + salubrinal treated cells was 4.98 ± 0.29 percent and 6.67 ± 1.74 percent at 1 μM concentration of rotenone respectively.

4. Discussion

In the present study, we have shown that salubrinal treatment significantly attenuated the rotenone induced NO mediated ER stress signaling, DNA damage and neuronal apoptosis. Previously also we have observed the rotenone induced reactive oxygen species generation, augmented nitrite level and impaired mitochondrial activity in both neuronal and glial cells (Goswami et al., 2011, 2014). It has been reported that salubrinal is selective inhibitor of eIF2alpha dephosphorylation and protects the cells from ER stress (Boyce et al., 2005; Duan et al., 2014) however it has also been reported that it could also offer neuroprotective effects through activation of other neuroprotective factors like NFkB (Huang et al., 2012). The present study showed the protective effects of salubrinal on the UPR related signaling factors along with other biochemical events. We have also observed that salubrinal pretreatment significantly inhibited the rotenone induced mitochondria mediated decreased cell viability and increased cytotoxicity. Previous studies have also showed that rotenone treatment caused the oxidative stress mediated apoptotic death of cells (Chen et al., 2008; Siddiqui et al., 2013). In the present study we have observed that the augmented 3-nitrotyrosine and nitrite levels were inhibited with aminoguanidine (AG) at given dose. Further, to assess the role of NO in observed ER stress the cells were co-treated with AG at selected dose. Co-treatment of AG with rotenone significantly inhibited the rotenone induced increased nitrite level and increased levels of ER stress markers namely GRP78, GADD153, cleaved caspae-12 and terminal executor of apoptotic death, cleaved caspase-3. Co-treatment of AG and pretreatment of salubrinal with rotenone also significantly inhibited the rotenone induced increased 3-nitrotyosine protein level. Such AG mediated

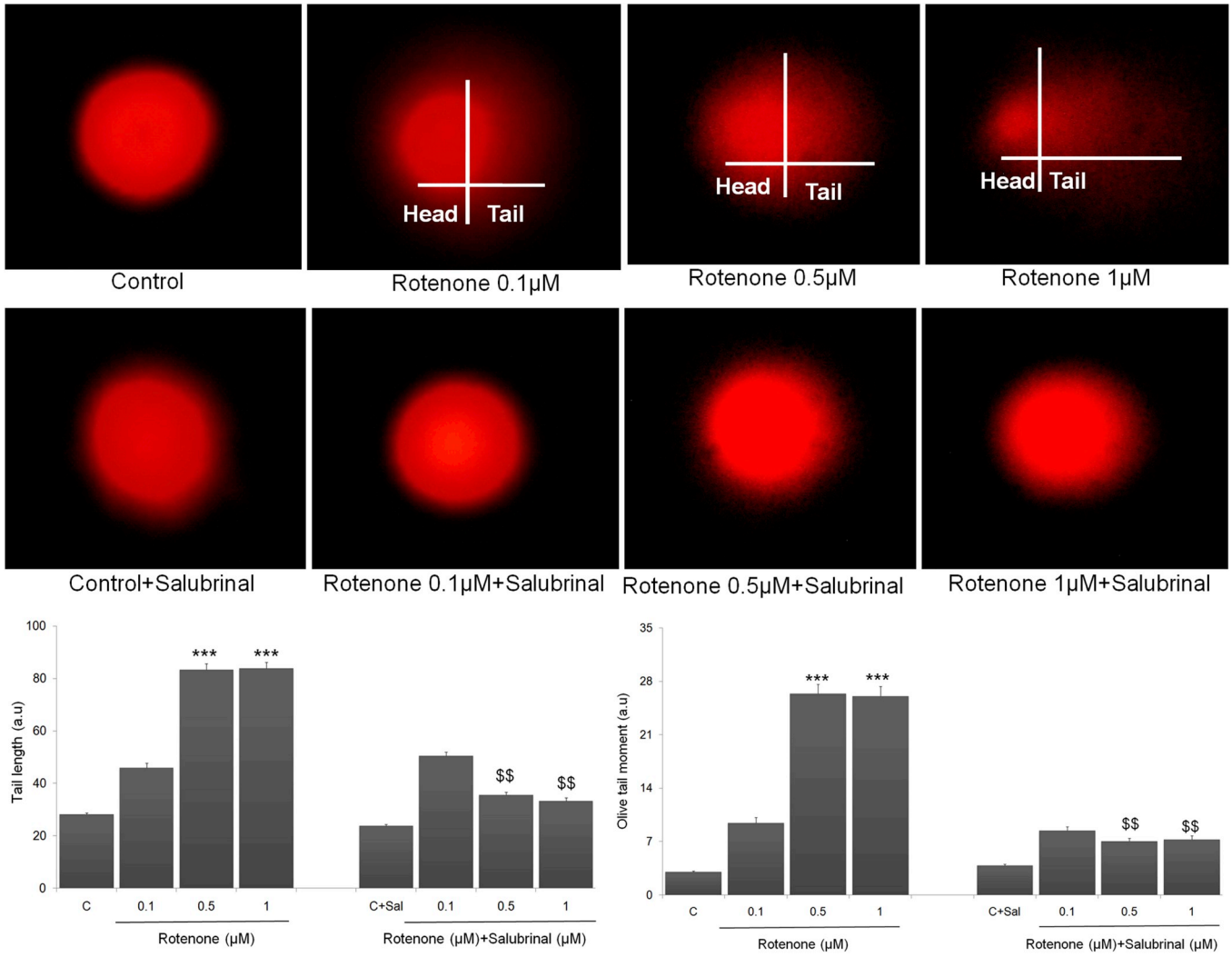

Fig. 6b. DNA fragmentation. Comet pictures showing DNA damage in neuro2A cells after rotenone and rotenone + salubrinal treatment. Graphical representation of the DNA damage assessed through the tail length and olive tail moment. Data are expressed as mean ± SEM and analyzed by ANOVA post hoc Newman Keuls Multiple Comparison Test. *** = $p < 0.001$ (control vs. Rotenone treated). $$ = $p < 0.01$ (Rotenone treated vs. Rotenone + Salubrinal treated.).

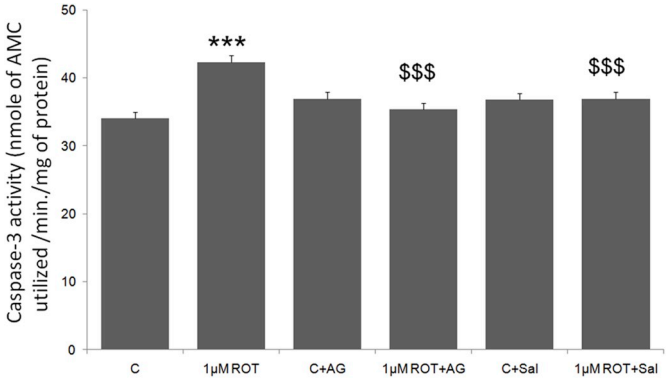

Fig. 6c. Caspase-3 activity in cells. Bar diagram representing the caspase-3 activity after 24 h of rotenone, rotenone + aminoguanidine (AG) and rotenone + salubrinal (Sal) treatment in neuro2A cells. Data are expressed as mean ± SEM, analyzed by ANOVA post hoc Newman-Keuls multiple comparison test. *** = $p < 0.001$ (Control vs. Rotenone treated). $$$ = $p < 0.001$ (Rotenone treated vs. Rotenone + Aminoguanidine treated.) $$$ = $p < 0.001$ (Rotenone treated vs. Rotenone + Salubrinal treated).

inhibition against rotenone induced ER stress markers suggested the pivotal role of NO in observed ER stress and apoptotic death of neurons. In ER stress the chaperon GRP78 plays an initiatory role as its dissociation from PERK, IRE1 and ATF6 offers their activation and consequently activate UPR (Liu and Kaufman., 2003; Luo and Lee, 2013; Wang et al., 2009; Zhu and Lee, 2015; Bravo et al., 2013). The observed increased level of GRP78 suggested its dissociation from the ER membrane located transmembrane kinases (PERK and IRE1) and activating transcription factors 6 (ATF6) and initiation of UPR. In concordance to this we have observed the augmented level of p-PERK, ATF4, p-IRE1α, XBP1, ATF6, GADD153, cleaved caspase12 and cleaved caspase3. However, the basal level of PERK and IRE1 was not altered. We have also observed the decreased level of phosphorylated eIF2α which is required to arrest the cellular translation to regulate the accumulation of misfolded proteins. Salubrinal is known inhibitor of eIF2α phosphatase enzymes however, its effects on other UPR related signaling factors are not known. We have observed that salubrinal treatment could attenuate the rotenone induced augmented level of p-PERK, ATF4, p-IRE1α, XBP1, ATF6, GADD153, cleaved caspase12 and cleaved caspase3 thus inhibit the ER stress and neuronal apoptosis. Earlier reports have also showed that pathological conditions involving accumulation of misfolded or unfolded protein caused the increased expression of GRP-78 and subsequent ER stress (Fonseca et al., 2013; Ding

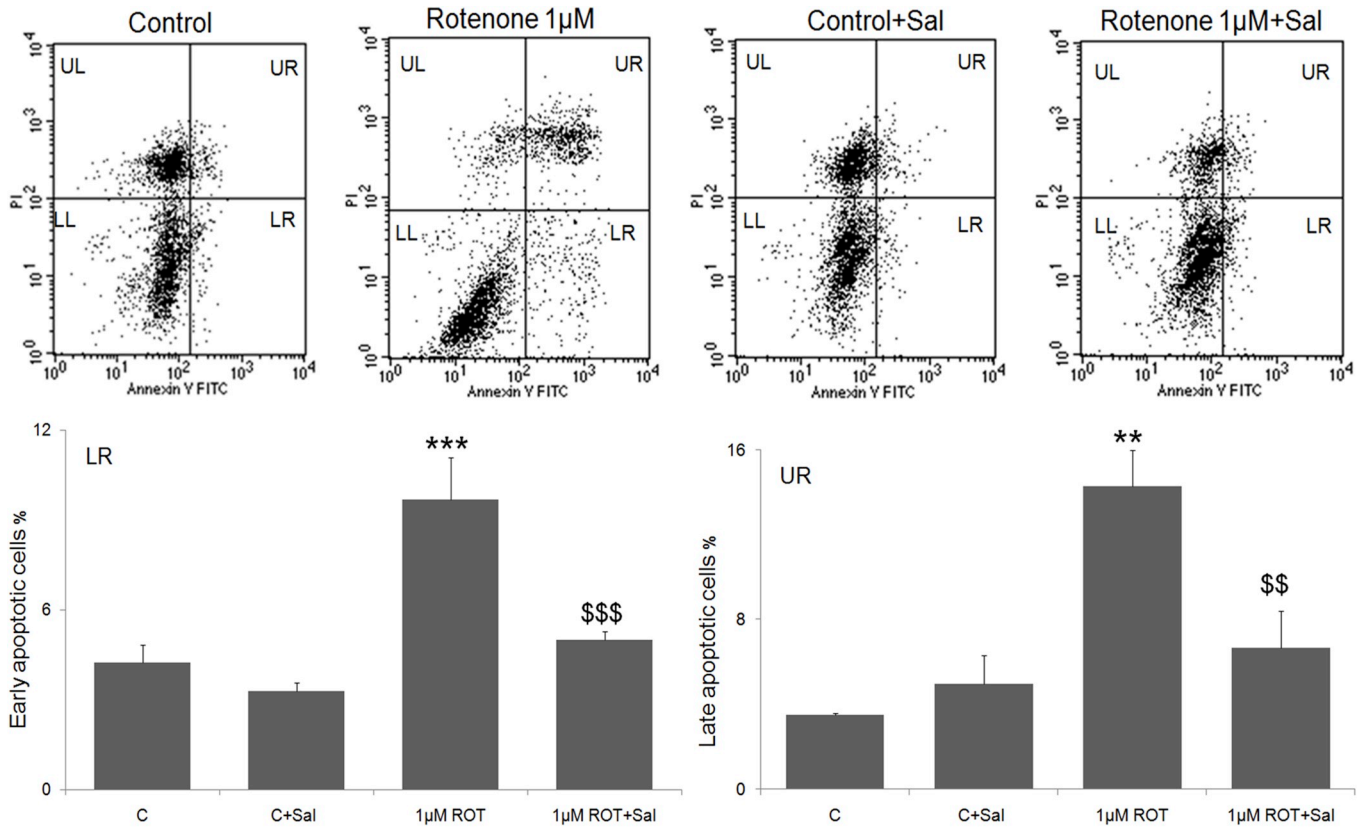

Fig. 6d. Annexin/PI staining in cells. **(a)** Representative images of Annexin/PI staining in neuro2A cells analyzed by flow cytometry **(b)** Graphical representation of Annexin/PI staining to assess cell death after rotenone treatment for 24 h in neuro2A cells. Data are expressed as mean ± SEM and analyzed by ANOVA post hoc Newman-Keuls multiple comparison test. ** = $p < 0.01$, *** = $p < 0.001$ (Control vs. Rotenone treated). $$ = $p < 0.01$, $$$ = $p < 0.001$ (Rotenone treated vs. Rotenone + Salubrinal treated).

et al., 2012). Various studies have detected the phosphorylated PERK and dephosphorylated eIF2α in substantia nigra pars compacta of human post-mortem parkinsonian brains (Smith and Mallucci., 2016; Hoozemans et al., 2009; Slodzinski et al., 2009). It has also been reported that increased level of dephosphorylated eIF2α caused the accumulation and aggregation of misfolded protein in ER which could trigger the apoptosis with increased expression of GADD153, caspase-12 and subsequent activation of caspase-3 and consequent neuronal apoptosis (Nakagawa and Yuan, 2000; Jason et al., 2009). In this context we have observed the augmented level of GADD153 and cleaved caspase 12 which were significantly attenuated with salubrinal treatment suggesting the salubrinal mediated regulation of GADD153 levels.

Direct link between the augmented level of ROS and cellular events like protein oxidation and protein folding has been suggested earlier (Higa and Chevet., 2012). It has also been reported that 6-OHDA mediated dopaminergic cell death proceeds through ROS dependent up regulation of UPR including impaired mitochondrial activity and apoptosis (Holtz et al., 2006). Oxidative stress mediated protein oxidation also contribute to ER stress mediated neuronal death (Malhotra and Kaufman., 2007). Therefore, the level of ROS was estimated in rotenone treated neuro2a cells. Significant ROS generation was observed in rotenone treated neuronal cells which was attenuated with salubrinal pretreatment. Previously also we and others have reported the rotenone induced ROS generation in neurons (Swarnkar et al., 2010; Goswami et al., 2015; Seoposengwe et al., 2013; Gupta et al., 2015a,b). Such augmented ROS level may be due to impaired mitochondrial activity which may further cause the initiation of various death signaling pathways (Yang et al., 2014; Hirst et al., 2008; Browning and Horton, 2004). Therefore, the MMP level was estimated after rotenone treatment to neuro2a cells. The MMP level was significantly diminished in rotenone treated neuro2a cells, which was significantly attenuated with salubrinal pretreatment. In concordance to our observation other reports are available showed the depleted MMP in astroglial cells after neurotoxins treatment (Biswas et al., 2016; Deng et al., 2013; Huang et al., 2016). Mitochondria also play a dual role in calcium homeostasis related cellular toxicity (Fulvio et al., 2009; Giorgi et al., 2012). Since we have observed the ROS generation, nitrosative stress and depleted MMP, further the intracellular calcium level was estimated. Rotenone treatment to neuronal cells caused the significantly increased level of calcium which was attenuated with salubrinal pretreatment. Increased cytosolic calcium levels can further trigger the free radical formation, lipid peroxidation and apoptosis as observed previously in both in vitro and in vivo test systems and contribute in neuronal death (Wang and Xu et al., 2005; Nicotera and Orrenius, 1998).

Such increased level of ROS, nitrite and intracellular calcium are directly related to chromatin condensation, DNA fragmentation and caspase mediated neuronal death (Brown and Borutaite, 2001 Bertram and Hass, 2008; Swarnkar et al., 2010; Rao, 2009; Barzilai, 2010). Therefore, the chromatin condensation, DNA fragmentation and neuronal apoptosis were estimated after rotenone treatment to neuronal cells. Rotenone treatment to neuro2a cells caused significantly increased chromatin condensation and DNA fragmentation in concentration dependent manner which was attenuated with pretreatment of salubrinal. Since caspase-3 is the primary activator of apoptotic DNA fragmentation, and considered as terminal executor of apoptotic pathway (Wolf et al., 1999; Singh and Dikshit, 2007) the caspase-3 activity was also estimated in cells. Findings indicated that rotenone treatment to neuro2a cells caused the significantly increased level of caspase-3 activity which was considerably attenuated with treatment of amninoguanidine as well as of salubrinal. Further, we also determine

the percentage of early and late apoptotic cellular population by fluorescence-activated cell sorting. Observation suggested that pretreatment of salubrinal confers protection to both early and late apoptosis in cells. Other reports have also demonstrated the induction of apoptosis and DNA fragmentation in primary neuronal cells by other environmental neurotoxins (Radad et al., 2006; Wiseman and Halliwell et al., 1996; Ohgoh et al., 2000; Yamazaki et al., 2006). GADD153 is a DNA damage inducible gene and the observed augmented level of GADD153 further supports the finding of DNA fragmentation. The observed increased level of GADD153 also contributes to disturbed redox state of cell through depletion of cellular glutathione and apoptosis as reported previously (Friedman, 1996; McCullough et al., 2001).

In conclusion, the findings of the present study indicated that rotenone treatment caused the decreased cell viability, oxidative stress, nitrosative stress, depleted mitochondrial activity, ER stress, up regulated UPR, DNA fragmentation, chromatin condensation, increased caspase-3 activity and neuronal apoptosis. Such rotenone induced adverse effects were significantly attenuated with pretreatment of salubrinal. Findings have also suggested that the rotenone induced ER stress was NO mediated and salubrinal is able to interfere in the rotenone induced altered level of various UPR related signaling factors. In addition findings have also indicated that the eIF2α may be considered in therapeutics of neurodegenerative diseases specifically related to accumulation of misfolded proteins like Parkinson's and Alzheimer's disease. Moreover, findings have suggested that salubrinal does not solely protect the cell through inhibition of eIF2alpha dephosphorylation but it could also interrupt the other degenerative pathways.

Acknowledgement

Author Sonam Gupta is thankful to the Indian Council of Medical Research (ICMR), India, for senior research fellowship and Academy of Scientific and Innovative Research (AcSIR) for providing opportunity to conduct research at CSIR-CDRI.

Authors are thankful to Department of Science and Engineering Board for providing financial support by research grant EMR/2015/001282.

Appendix A. Supplementary data

Supplementary data to this article can be found online at https://doi.org/10.1016/j.neuint.2019.104581.

References

B'chir, W., Maurin, A.C., Carraro, V., Averous, J., Jousse, C., Muranishi, Y., Parry, L., Stepien, G., Fafournoux, P., Bruhat, A., 2013. The eIF2α/ATF4 pathway is essential for stress-induced autophagy geneexpression. Nucleic Acids Res. 41, 7683–7699.

Barzilai, A., 2010. DNA damage, neuronal and glial cell death and neurodegeneration. Apoptosis 15, 1371–1381.

Bertram, C., Hass, R., 2008. Cellular responses to reactive oxygen species-inducedDNA damage and aging. Biol. Chem. 389, 211–220.

Biswas, J., Goswami, P., Gupta, S., Joshi, N., Nath, C., Singh, S., 2016. Streptozotocin induced neurotoxicity involves Alzheimer's related pathological markers: a study on N2A cells. Mol. Neurobiol. 53, 2794–2806.

Boyce, M., Bryant, K.F., Jousse, C., Long, K., Harding, H.P., Scheuner, D., Kaufman, R.J., Ma, D., Coen, D.M., Ron, D., Yuan, J., 2005. A selective inhibitor of eIF2alpha dephosphorylation protects cells from ER stress. Science 307, 935–939.

Bravo, R., Parra, V., Gatica, D., Rodriguez, A.E., Torrealba, N., Paredes, F., Wang, Z.V., Zorzano, A., Hill, J.A., Jaimovich, E., Quest, A.F., Lavandero, S., 2013. Endoplasmic reticulum and the unfolded protein response: dynamics and metabolicintegration. Int. Rev. Mol. Cell Biol. 301, 215–290.

Brorson, J.R., Zhang, H., 1997. Disrupted [Ca2+]i homeostasis contributes to thetoxicity of nitric oxide in cultured hippocampal neurons. J. Neurochem. 69, 1882–1889.

Brown, G.C., Borutaite, V., 2001. Nitric oxide, mitochondria, and cell death. IUBMB Life 52, 189–195.

Browning, J.D., Horton, J.D., 2004. Molecular mediators of hepatic steatosis and liver injury. J. Clin. Investig. 114, 147–152.

Chen, Y.Y., Chen, G., Fan, Z., Luo, J., Ke, Z.J., 2008. GSK3beta and endoplasmic reticulum stress mediate rotenone-induced death of SK-N-MC neuroblastoma cells. Biochem. Pharmacol. 76, 128–138.

Chung, J., Kim, K.H., Lee, S.C., An, S.H., Kwon, K., 2015. Ursodeoxycholic acid (UDCA) exerts anti-atherogenic effects by inhibiting endoplasmic reticulum (ER) stress induced by disturbed flow. Mol. Cells 38, 851–858.

Corazzari, M., Gagliardi, M., Fimia, G.M., Piacentini, M., 2017. Endoplasmic reticulum stress, unfolded protein response, and cancer CellFate. Front. Oncol. 26, 7–78.

Deng, Y.N., Shi, J., Liu, J., Qu, Q.M., 2013. Celastrol protects human neuroblastoma SH-SY5Y cells from rotenone-induced injury through induction of autophagy. Neurochem. Int. 63, 1–9.

Dickhout, J.G., Hossain, G.S., Pozza, L.M., Zhou, J., Lhoták, S., Austin, R.C., 2005. Peroxynitrite causes endoplasmic reticulum stress and apoptosis in human vascular endothelium: implications in atherogenesis. Arterioscler. Thromb. Vasc. Biol. 25, 2623–2629.

Ding, W., Yang, L., Zhang, M., Gu, Y., 2012. Reactive oxygen species-mediated endoplasmicreticulum stress contributes to aldosterone-induced apoptosis in tubular epithelial cells. Biochem. Biophys. Res. Commun. 418, 451–456.

Duan, Z., Zhao, J., Fan, X., Tang, C., Liang, L., Nie, X., Liu, J., Wu, Q., Xu, G., 2014. The PERK-eIF2α signaling pathway is involved in TCDD-induced ERstress in PC12 cells. Neurotoxicology (Little Rock) 44, 149–159.

Esposito, E., Iacono, A., Muia, C., Crisafulli, C., Mattace-Raso, G., Bramanti, P., Meli, R., Cuzzocrea, S., 2008. Signal transduction pathways involved in protectiveeffects of melatonin in C6 glioma cells. J. Pineal Res. 44, 78–87.

Fonseca, A.C., Ferreiro, E., Oliveira, C.R., Cardoso, S.M., Pereira, C.F., 2013. Activation of the endoplasmic reticulum stress response by the amyloid-beta 1-40 peptide in brain endothelial cells. Biochim. Biophys. Acta 1832, 2191–2203.

Friedman, A.D., 1996. GADD153/CHOP, a DNA damage-inducible protein, reduced CAAT/enhancer binding protein activities and increased apoptosis in 32D c13 myeloid cells. Cancer Res. 15, 3250–3256.

Fulvio, Celsi, Paola, Pizzo, Marisa, Brini, Sara, Leo, Carmen, Fotino, Paolo, Pinton, Rosario, Rizzuto, 2009. Mitochondria, calcium and cell death: a deadly triad in neurodegeneration Biochimica et Biophysica Acta (BBA). Bioenergetics 335–344.

Giorgi, Carlotta, Agnoletto, Chiara, Bononi, Angela, Bonora, Massimo, De Marchi, Elena, Marchi, Saverio, Missiroli, Sonia, Patergnani, Simone, Poletti, Federica, Rimessi, Alessandro, Suski, Jan M., Wieckowski, Mariusz R., Pinton, Paolo, 2012. Mitochondrial calcium homeostasis as potential target for mitochondrial medicine. Mitochondrion 12, 77–85.

Goswami, Poonam, Swarnkar, Supriya, Mohmed Sohail Harsoliya,Singh, Sarika, Nath, Chandishwar, Sharma, Sharad, 2011. Attenuation of DNA damage: a key step in neuroprotective effect of piracetam against 6-hydroxydopamine induced neuronal death in SHSY5Y cells. J. Pharm. Res. 4, 1716–1719.

Goswami, P., Gupta, S., Biswas, J., Joshi, N., Swarnkar, S., Nath, C., Singh, S., 2014. Endoplasmic reticulum stress plays a key role in rotenone-induced apoptotic death of neurons. Mol. Neurobiol. 53, 285–298.

Goswami, P., Gupta, S., Biswas, J., Sharma, S., Singh, S., 2015. Endoplasmic reticulum stress instigates the rotenone induced oxidative apoptotic neuronal death: a study in rat brain. Mol. Neurobiol. 53, 5384–5400.

Gupta, S., Verma, D.K., Biswas, J., Rama Raju, K.S., Joshi, N., Wahajuddin, Singh, S., 2014. The metabolic enhancer piracetam attenuates mitochondrion-specific endonuclease G translocation and oxidative DNA fragmentation. Free Radic. Biol. Med. 73, 278–290.

Gupta, S., Goswami, P., Biswas, J., Joshi, N., Sharma, S., Nath, C., Singh, S., 2015a. 6-Hydroxydopamine and lipopolysaccharides induced DNA damage in astrocytes: involvement of nitric oxide and mitochondria. Mutat. Res. Genet. Toxicol. Environ. Mutagen. 778, 22–36.

Gupta, S., Goswami, P., Joshi, N., Sharma, S., Singh, S., 2015b. Astrocyte activation and neurotoxicity: a study in different rat brain regions and in rat C6 astroglial cells. Environ. Toxicol. Pharmacol. 778, 22–36.

Hail, N., Lotan Jr., R., 2000. Mitochondrial permeability transition is a centralcoordinating event in N-(4-hydroxyphenyl) retinamide-induced apoptosis. Cancer Epidemiol. Biomark. Prev. 9, 1293–1301.

Haze, K., Yoshida, H., Yanagi, H., Yura, T., Mori, K., 1999. Mammalian transcription factor ATF6 is synthesized as a transmembrane protein and activated by proteolysis in response to endoplasmic reticulum stress. Mol. Biol. Cell 10, 3787–3799.

Higa, A., Chevet, E., 2012. Redox signaling loops in the unfolded protein response. Cell. Signal. 24, 1548–1555.

Hirst, J., King, M.S., Pryde, K.R., 2008. The production of reactive oxygen species by complex I. Biochem. Soc. Trans. 36, 976–980.

Holtz, W.A., Turetzky, J.M., Jong, Y.J., O'Malley, K.L., 2006. Oxidative stress-triggered unfolded protein response is upstream of intrinsic cell death evoked by parkinsonian mimetics. J. Neurochem. 99, 54–69.

Hoozemans, J.J., van Haastert, E.S., Nijholt, D.A., Rozemuller, A.J., Eikelenboom, P., 2009. The unfolded protein response is activated in pretangle neurons in Alzheimer's disease hippocampus. Am. J. Pathol. 174, 1241–1251.

Huang, G., Yao, J., Zeng, W., Mizuno, Y., Kamm, K.E., Stull, J.T., Harding, H.P., Ron, D., Muallem, S., 2006. ER stress disrupts Ca2+-signaling complexes and Ca2+ regulation in secretory and muscle cells from PERK-knockout mice. J. Cell Sci. 1, 153–161.

Huang, X., Chen, Y., Zhang, H., Ma, Q., Zhang, Y.W., Xu, H., 2012. Salubrinal attenuates beta-amyloid-induced neuronal death and microglial activation by inhibition of the NF-kappaB pathway. Neurobiol. Aging 33, 9–17.

Huang, J.Y., Yuan, Y.H., Yan, J.Q., Wang, Y.N., Chu, S.F., Zhu, C.G., Guo, Q.L., Shi, J.G., Chen, N.H., 2016. A bibenzyl compound isolated from Gastrodia elata, protects PC12 cells against rotenone-induced apoptosis via activation of the Nrf2/ARE/HO-1 signaling pathway. Acta Pharmacol. Sin. 37, 731–740.

Jason, B., Lee, W., Karen, S., Poksay, Brian, N., Bredesen, Dale E., Rammohan, V. Rao, 2009. Coupling endoplasmicreticulumstress to thecell death program in mouse melanoma cells:effect of curcumin. Apoptosis 13, 904–914.

Jeon, Y.M., Lee, S., Kim, S., Kwon, Y., Kim, K., Chung, C.G., Lee, S., Lee, S.B., Kim, H.J., 2017. Neuroprotective effects of protein tyrosine phosphatase 1B inhibition against

ER stress-inducedtoxicity. Mol. Cells 40, 280–290.
Jing, Xiuna, Shi, Qiaoyun, Bi1, Wei, Zeng, Zhifen, Liang, Yanran, Wu, Xia, Xiao1, Songhua, Liu, Jun, Yang, Lianhong, Tao, Enxiang, 2014. Rifampicin protects PC12 cells from rotenone-induced cytotoxicity by activating GRP78 via PERK-eIF2α-ATF4 pathway. Crit. Rev. Toxicol. 42, 613–632.
Lange, P.S., Chavez, J.C., Pinto, J.T., Coppola, G., Sun, C.W., Townes, T.M., Geschwind, D.H., Ratan, R.R., 2008. ATF4 is an oxidative stress-inducible, prodeath transcription factor in neuronsin vitro and in vivo. J. Exp. Med. 12, 1227–1242.
Li, N., Ragheb, K., Lawler, G., Sturgis, J., Rajwa, B., Melendez, A.J., Robinson, J.P., 2003. Mitochondrial complex I inhibitor rotenone induces apoptosis through enhancing mitochondrial reactive oxygen species production. J. Biol. Chem. 278, 8516–8525.
Li, Y., Guo, Y., Tang, J., Jiang, J., Chen, Z., 2014. New insights into the roles of CHOP-induced apoptosis in ER stress. Acta Biochim. Biophys. 46, 629–640.
Liu, C.Y., Kaufman, R.J., 2003. The unfolded protein response. J. Cell Sci. 15, 1861–1862.
Liu, X., Kim, C.N., Yang, J., Jemmerson, R., Wang, X.D., 1996. Induction of apoptotic program in cell-free extracts: requirement for dATP and cytochrome c. Cell 86, 147–157.
Liu, C.L., Li, X., Hu, G.L., Li, R.J., He, Y.Y., Zhong, W., Li, S., He, K.L., Wang, L.L., 2012. Salubrinal protects against tunicamycin and hypoxia induced cardiomyocyte apopto sis via the PERK-eIF2α signaling pathway. J. Geriatr. Cardiol. 9, 258–268.
Lowry, O.H., Rosebrough, N.J., Farr, A.I., Randall, R.J., 1951. Protein measurement with the Folin phenol reagent. J. Biol. Chem. 193, 265–275.
Luo, B., Lee, A.S., 2013. The critical roles of endoplasmic reticulum chaperones and unfolded protein response in tumorigenesis and anti-cancer therapies. Oncogene 32. https://doi.org/10.1038/onc.2012.130.
Malhotra, J.D., Kaufman, R.J., 2007. Endoplasmic reticulum stress and oxidative stress: a vicious cycle or a double-edged sword? Antioxidants Redox Signal. 9, 2277–2293.
Matsuoka, Masato, Komoike, Yuta, 2015. Experimental evidence shows salubrinal, an eIF2α dephosphorylation inhibitor, reduces xenotoxicant-induced cellular damage. Int. J. Mol. Sci. 16, 16275–16287.
McCullough, K.D., Martindale, J.L., Klotz, L.O., Aw, T.Y., Holbrook, N.J., 2001. Gadd153 sensitizes cells to endoplasmic reticulum stress by down-regulating Bcl2 and perturbing the cellular redox state. Mol. Cell. Biol. 21, 1249–1259.
Methippara, M., Mitrani, B., Schrader, F.X., Szymusiak, R., McGinty, D., 2012. Salubrinal, an endoplasmic reticulum stress blocker, modulates sleep homeostasis and activation of sleep-and wake-regulatory neurons. Neuroscience 209, 108–118.
Nakagawa, T., Yuan, J., 2000. Cross-talk between two cysteine protease families: activation of caspase-12 by calpain in apoptosis. J. Cell Biol. 150, 887–894.
Nicotera, P., Orrenius, S., 1998. The role of calcium in apoptosis. Cell Calcium 23, 173–180.
Nishitoh, H., 2012. CHOP is a multifunctional transcription factor in the ER stress response. J. Biochem. 151, 217–219.
Ohgoh, M., Shimizu, H., Ogura, H., Nishizawa, Y., 2000. Astroglial trophic support and neuronal cell death: influence of cellular energy level on type of cell death induced by mitochondrial toxin in cultured rat cortical neurons. J. Neurochem. 75, 925–933.
Ohno, M., 2014. Roles of eIF2α kinases in the pathogenesis of Alzheimer's disease. Front. Mol. Neurosci. 16, 7–22.
Oyadomari, S., Mori, M., 2004. Roles of CHOP/GADD153 in endoplasmic reticulum stress. Cell Death Differ. 11, 381–389.
Paschen, W., 2003. Endoplasmic reticulum: a primary target in various acute disorders and degenerative diseases of the brain. Cell Calcium 34, 365–383.
Radad, K., Rausch, W.D., Gille, G., 2006. Rotenone induces cell death in primary dopaminergic culture by increasing ROS production and inhibiting mitochondrial respiration. Neurochem. Int. 49, 379–386.
Rao, K.S., 2009. Free radical induced oxidative damage to DNA: relation to brainaging and neurological disorders. Indian J. Biochem. Biophys. 46, 9–15.
Ron, D., Hubbard, S.R., 2008. How IRE1 reacts to ER stress. Cell 11, 24–26.
Rutkowski, D.T., Hegde, R.S., 2010. Regulation of basal cellular physiology by the homeostatic unfolded protein response. J. Cell Biol. 189, 783–794.
Seoposengwe, K., van Tonder, J.J., Steenkamp, V., 2013. In vitro neuroprotective potential of four medicinal plants against rotenoneinduced toxicity in SH-SY5Y neuroblastoma cells. BMC Complement Altern. Med. 13, 353–362.
Siddiqui, M.A., Ahmad, J., Farshori, N.N., Saquib, Q., Jahan, S., Kashyap, M.P., Ahamed, M., Musarrat, J., Al-Khedhairy, A.A., 2013. Rotenone-induced oxidative stress and apoptosis in human liver HepG2 cells. Mol. Cell. Biochem. 384, 59–69.
Singh, S., Dikshit, M., 2007. Apoptotic neuronal death in Parkinson's disease: involvement of nitric oxide. Brain Res. 54, 233–250.
Singh, S., Goswami, P., Swarnkar, S., Singh, S.P., Wahajuddin, Nath, C., Sharma, S., 2011. A study to evaluate the effect of nootropic drug-piracetam on DNA damage in leukocytes and macrophages. Mutat. Res. 726, 66–74.
Singh, S., Kumar, S., Dikshit, M., 2010. Involvement of mitochondrial apoptoticpathway and nitric oxide synthase in 6-hydroxydopamine and lipopolysacchride induced dopaminergic neuronal death. Redox Rep. 15, 1–8.
Slodzinski, H., Moran, L.B., Michael, G.J., Wang, B., Novoselov, S., Cheetham, M.E., Pearce, R.K., Graeber, M.B., 2009. Homocysteine-induced endoplasmic reticulum protein (herp) is up-regulated in Parkinsonian substantia nigra and present in the core of Lewy bodies. Clin. Neuropathol. 28, 333–343.
Smith, H.L., Mallucci, G.R., 2016. The unfolded proteinresponse: mechanisms and therapy of neurodegeneration. Brain 139, 2113–2121.
Susin, S., Lorenzo, H., Zamzami, N., Marzo, I., Brenner, C., Larochette, N., Prevost, M., Alzari, P., Kroemer, G., 1999. Mitochondrial release of caspase-2 and-9 during the apoptotic process. J. Exp. Med. 189, 381–394.
Swarnkar, S., Goswami, P., Kumar, K.P., Gupta, S., Patro Ishan, K., Singh, S., Nath, C., 2012. Rotenone-induced apoptosis and role of calcium: a study on Neuro-2a cells. Arch. Toxicol. 86, 1387–1397.
Swarnkar, S., Singh, S., Mathur, R., Patro, I.K., Nath, C., 2010. A study to correlate rotenone induced biochemical changes and cerebral damage in brain areas with neuromuscular coordination in rats. Toxicology 272, 17–22.
Takada, K., Hirose, J., Yamabe, S., Uehara, Y., Mizuta, H., 2013. Endoplasmic reticulum stress mediates nitric oxide-induced chondrocyte apoptosis. Biomed. Rep. 1, 315–319.
Walter, Peter, Ron, David, 2011. The unfolded protein response: from stress pathway to homeostatic regulation. Science 334, 1081–1086.
Wang, X.J., Xu, J.X., 2005. Possible involvement of Ca2? signaling in rotenone-induced apoptosis in human neuroblastoma SH-SY5Y cells. Neurosci. Lett. 376, 127–132.
Wang, Miao, Wey, Shiuan, Zhang, Yi, Ye, Risheng, Amy, S., Lee, 2009. Role of the unfolded protein response regulator GRP78/BiP in development, cancer, and neurological disorders. Antioxidants Redox Signal. 11, 2307–2316.
Watabe, M., Nakaki, T., 2004. Rotenone induces apoptosis via activation of bad in human dopaminergic SH-SY5Y cells. J. Pharmacol. Exp. Ther. 311, 948–953.
Wiseman, H., Halliwell, B., 1996. Damage to DNA by reactive oxygen and nitrogen species: role in inflammatory disease and progression to cancer. Biochem. J. 313, 17–29.
Wolf, B.B., Schuler, M., Echeverri, F., Green, D.R., 1999. Caspase-3 is the primary activator of apoptotic DNA fragmentation via DNA fragmentation factor-45/inhibitor of caspase-activated DNase inactivation. J. Biol. Chem. 274, 30651–30656.
Wu, C.T., Sheu, M.L., Tsai, K.S., Chiang, C.K., Liu, S.H., 2011. Salubrinal, an eIF2α dephosphorylation inhibitor, enhances cisplatin-induced oxidative stress and nephrotoxicity in a mouse model. Free Radic. Biol. Med. 51, 671–680.
Wroblewski, F., Laude, J.S., 1955. Lactic dehydrogenase activity in blood. Proc. Soc. Exp. Biol. Med. 90, 210–213.
Xu, C., Bailly-Maitre, B., Reed, J.C., 2005. Endoplasmic reticulum stress: cell life and death decisions. J. Clin. Investig. 115, 2656–2664.
Xu, S.Y., Hu, Y.F., Li, W.P., Wu, Y.M., Ji, Z., Wang, S.N., Li, K., Pan, S.Y., 2014. Intermittent hypothermia is neuroprotective in an in vitro model of ischemic stroke. Int. J. Biol. Sci. 10, 873–881.
Yamazaki, T., Muramoto, M., Oe, T., Morikawa, N., Okitsu, O., Nagashima, T., Nishimura, S., Katayama, Y., Kita, Y., 2006. Diclofenac, a non-steroidal anti-inflammatory drug, suppresses apoptosis induced by endoplasmic reticulum stresses by inhibiting caspase signaling. Neuropharmacology 50, 558–567.
Yang, J.T., Li, Z.L., Wu, J.Y., Lu, F.J., Chen, C.H., 2014. An oxidative stress mechanism of shikonin in human glioma cells. PLoS One 8 (9), e94180 4.
Zhu, G., Lee, A.S., 2015. Role of the unfolded protein response, GRP78 and GRP94 in organ homeostasis. J. Cell. Physiol. 230, 1413–1420.
Zong, W.X., Li, C., Hatzivassiliou, G., Lindsten, T., Yu, Q.C., Yuan, J., Thompson, C.B., 2003. Bax and Bak can localize to the endoplasmic reticulum to initiate apoptosis. J. Cell Biol. 7, 59–69.